


Article

Source Profile Analysis, Source Apportionment, and Potential Health Risk of Ambient Particle-Bound Polycyclic Aromatic Hydrocarbons in Areas of Specific Interest

Dikaia Saraga , Michail Pachoulis , Maria Dasopoulou, Panagiotis Panagopoulos, Dimitra Balla , Kyriaki Bairachtari and Thomas Maggos * 

Atmospheric Chemistry & Innovative Technologies Laboratory, INRASTES, NCSR Demokritos, Aghia Paraskevi, 15310 Athens, Greece; dsaraga@ipta.demokritos.gr (D.S.); m.pachoulis@ipta.demokritos.gr (M.P.); mdasopoulou@ipta.demokritos.gr (M.D.); p.panagopoulos@ipta.demokritos.gr (P.P.); ballad@ipta.demokritos.gr (D.B.); kbairaki@gmail.com (K.B.)

* Correspondence: tmaggos@ipta.demokritos.gr; Tel.: +30-21-0650-3716

Abstract: Ambient particulate matter (PM₁₀) and its chemical composition in polycyclic aromatic hydrocarbons (PAHs) were studied in areas of specific interest, between September 2015 and July 2016. The principal aim of this study was to assess the different PAH source profiles in each area, as well as their potential health risk. In particular, the studied areas were (a) the semiurban industrialized zone of the Municipality of Peloponnese (Meligalas, Messini) of Messinia prefecture, due to the intensive olive-productive activity in the extensive area, (b) the industrialized zone of Oinofyta in Voiotia prefecture, and (c) the urban/traffic center of Athens (Aristotelous). Intense spatial and seasonal variations in PAH levels were observed among the study areas collectively, but also for each one individually. During the winter period, the total PAHs average concentration was 11.45 and 9.84 ng/m³ at Meligalas–Skala (S1, S2 stations), 8.84 ng/m³ at Messini (S3 station), and 6.30 ng/m³ at the center of Athens (Aristotelous). During the summer campaign, the corresponding levels were 0.99, 1.20, and 0.70 ng/m³ (S1, S2, and S3 stations), and 5.84 ng/m³ (Aristotelous), respectively. The highest potential cancer risk of the PAHs mixture was estimated based on winter season measurements taken at the Municipality of Peloponnese. In order to determine PAH sources, two different source apportionment techniques were applied, i.e., diagnostic ratios (DRs) and the positive matrix factorization (PMF) model.

Keywords: PAHs; kernel olive industries; diagnostic ratios; PMF; risk assessment; source identification; air quality



Citation: Saraga, D.; Pachoulis, M.; Dasopoulou, M.; Panagopoulos, P.; Balla, D.; Bairachtari, K.; Maggos, T. Source Profile Analysis, Source Apportionment, and Potential Health Risk of Ambient Particle-Bound Polycyclic Aromatic Hydrocarbons in Areas of Specific Interest. *Atmosphere* **2024**, *15*, 938. <https://doi.org/10.3390/atmos15080938>

Academic Editor: Luca Stabile

Received: 1 July 2024

Revised: 25 July 2024

Accepted: 29 July 2024

Published: 5 August 2024



Copyright: © 2024 by the authors. Licensee MDPI, Basel, Switzerland. This article is an open access article distributed under the terms and conditions of the Creative Commons Attribution (CC BY) license (<https://creativecommons.org/licenses/by/4.0/>).

1. Introduction

In recent decades, much attention has been given to the study of airborne particulate matter (PM) due to its potential adverse effect on human health. According to the World Health Organization (WHO)'s update for 2023, worldwide air pollution is the greatest environmental threat to public health, causing 7 million premature deaths every year. In 2019, 99% of the world population was living in places where the WHO's strictest 2021 air quality guideline levels were not met [1]. Particulate matter (PM₁₀ and PM_{2.5}) is linked with several deadly illnesses, such as heart disease, stroke, respiratory mortality (COPD and acute lower respiratory infections, such as pneumonia), cardiovascular mortality (cerebrovascular disease and IHD), and chronic obstructive pulmonary diseases [2,3]. Numerous inorganic and organic compounds have been detected in PM₁₀, formed by a wide variety of mechanisms related to natural and anthropogenic sources. Much attention has been given to the organic fraction, and especially to persistent organic pollutants (POPs), including polycyclic aromatic hydrocarbons (PAHs), due to their potential to bioaccumulate and pose a risk of causing adverse effects to human health and the environment [4,5].

Consequently, an expanding body of research has concentrated on gathering additional data concerning PAHs, determining their sources, and assessing potential health impacts on humans, aiming to enhance the understanding of these complicated mechanisms. Source apportionment approaches comprise a robust method for characterizing and attributing the sources of PAHs [6]. An increasing number of studies have been directed towards urban areas due to human activities [7–10]. In addition, the spatial distribution of sources can yield crucial insights into pollutant dynamics, helping to identify different pollution patterns and develop control strategies to prevent health risks [11–14]. The relation between the air pollutants and health effects has been extensively documented in studies [15,16], including the indoor and outdoor exposure of children and adults to harmful substances [17–20].

PAHs are a class of complex organic chemicals which only include carbon and hydrogen arranged in two or more fused aromatic rings and are formed by the incomplete combustion of organic materials. The main emission sources of PAHs include residential combustion processes (open fires, coal and wood burning for heating purposes, etc.), industrial metal production processes, and the road transport sector. Their carcinogenic and mutagenic potential and their wide distribution mean that 16 PAHs have been included on the list of priority pollutants by the United States Environmental Protection Agency. Among them, Benzo[a]anthracene, Benzo[a]pyrene, dibenzo[a,h]anthracene, benzo[b]fluoranthene, benzo[k]fluoranthene, benzo[ghi]perylene, and indeno[1,2,3-cd]pyrene have been classified as probable human carcinogens. Benzo[a]pyrene (BaP) has been classified by the International Agency for Research on Cancer (IARC) as a known carcinogen to humans, and for this reason, it is used as an indicator of exposure to harmful PAHs [21]. Atmospheric PAHs can be distributed between the PM and gas phases. Lighter PAHs like naphthalene are predominantly present in the gas phase. On the other hand, heavier PAHs such as B[a]P are primarily absorbed onto particles. These findings suggest that particulate PAHs pose significant health hazards to the human respiratory system through inhalation. Furthermore, depending on atmospheric conditions, these PAHs may be airborne for days and transported over long distances, which is the reason why the pollution status of an area is considered as a mixed signature of both local and external sources.

Based on the above, and especially regarding health concerns, several studies have been focused on the identification of concentration levels and sources of these compounds. Studies indicate that the most significant concentration levels of PAHs have been observed for urban and industrialized areas rather than for rural areas [22]. For the determination of sources, receptor models have been widely used in different environments; among these, positive matrix factorization (PMF), chemical mass balance (CMB), and principal component analysis (PCA) have been used extensively for the identification of sources and estimation of the contribution of measured PM samples [23].

The present study aims to assess the variance of PAH concentrations, as well as to identify and quantify the contribution of pollution sources of these hazardous compounds in three areas with different characteristics. More specifically, an industrialized zone of Oinofyta, where several heavy industries (i.e., metallurgy and metal processing, chemical manufacturing, plastic production, food processing, textile manufacturing) are located, an area with intense olive-productive activity in the Peloponnese region, and an urban site with heavy traffic in the Athens city center were selected for an approximately 1-year sampling campaign. To the best of our knowledge, this study constitutes a first attempt to assess the impact of combined data from heavy industrial areas, olive-productive areas, and traffic-related urban environments on air quality and human health, specifically the carcinogenic equivalent concentration (TEQ). In addition, two source apportionment tools were applied on the collected data, i.e., the diagnostic ratios (DRs) and the PMF model, in order to identify the main PAH sources contributing to measured air pollution levels in each area.

2. Data and Methodology

2.1. Study Areas Characteristics

Sampling of ambient PM₁₀ was conducted in three areas with different kind of activities from September 2015 to July 2016 (Figure 1). The first sampling area includes the semiurban industrialized zone of the Municipality of Peloponnese in the Messinia Region, characterized by intensive olive production in the extensive area. Three monitoring stations were selected and positioned to cover the area where four olive pomace industries are located (Table A1). The sampling site (S1) was located to the north, while (S2) was situated to the south of the industries, in the Meligalas area. In Messini, site (S3) was located to the west of the industries (Figure 2).

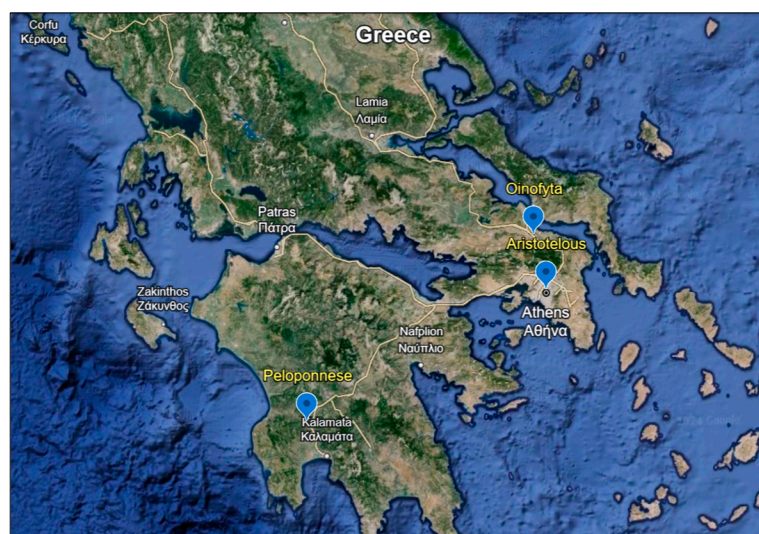


Figure 1. The sampling sites of Peloponnese, Aristotelous, and Oinofyta.



Figure 2. (a) The sampling sites S1, S2, and (b) S3 in Municipality of Peloponnese.

The second sampling area is the urban center of Athens (Figure 3). The sampling site (Y1) was located on the first floor of the Greek Ministry of Health, facing Aristotelous Street and a three-way junction characterized by dense vehicular traffic and commercial activity.

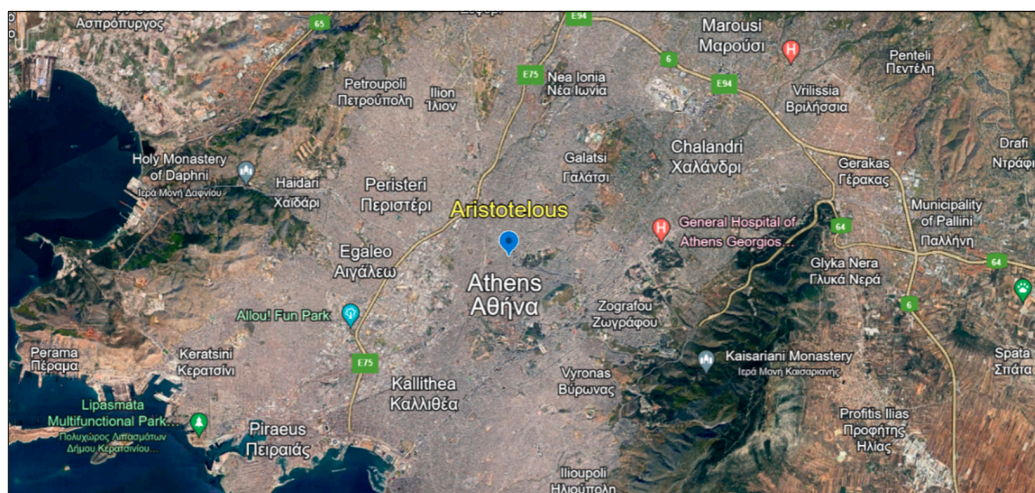


Figure 3. The sampling site Y1, Aristotelous in center of Athens.

The sampling area of Oinofyta in the Voiotia (Figure 4) prefecture is located in a highly industrialized zone, near the national highway. Four sampling sites (A1–A4) were selected across the area.



Figure 4. The sampling sites A1, A2, A3, and A4 in Oinofyta.

The number of samples collected at each sampling site during the campaigns was 45, 17, and 90 for the Municipality of Peloponnese, Oinofyta, and Aristotelous, respectively. The sampling period for the Municipality of Peloponnese was from 6 November 2015 to 1 April 2016. This period is characterized by intense activity of the olive pomace oil industries which contribute to poor air quality in the area. To achieve a more comprehensive recording of the targeted pollutants to provide a strongly documented scientific perspective, at the end of the operation of the olive pomace oil industries (November–March 2016), further sampling was performed (1–10 July 2016) to determine the level of background concentrations. For the Oinofyta area, the sampling campaign was conducted between 21 September 2015 and 20 October 2015, while for Aristotelous Street, it was conducted between 25 December 2015 and 6 March 2016 and again from 30 May 2016 to 20 July 2016. Table 1 summarizes the characteristics of each area and provides information on each sampling campaign.

Table 1. Summary information of sampling areas.

	Municipality of Oichalia–Messini (Peloponnese, Greece)	Oinofyta (Voiotia, Greece)	Aristotelous (Athens, Greece)
Sampling sites	Meligalas (S1) Skala (S2) Messini (S3)	A1 A2 A3 A4	Y1
Sampling period	November 2015–March 2016 July 2016	September– October 2015	December 2015–March 2016 May–July 2016
Number of samples	45	17	90
Area characteristics	Semiurban industrialized/ olive pomace-productive zone	Traffic/industrial zone	Traffic/urban center

2.2. Sampling and Analytical Techniques and Quality Control

At all sites, PM₁₀ sampling was conducted using low-volume samplers operating according to the specifications for PM₁₀ designated by the European EN12341:2014 (Ambient Air-Standard gravimetric measurement method for the determination of the PM₁₀ or the PM_{2.5} mass concentration of suspended particulate matter) [24]. The flow rate was set at 2.3 m³ h, and the operation time was 24 h. Ambient PM₁₀ was collected on microfiber quartz filters with diameters of 47 and 50 mm. Before sampling, filters were cleaned by thermal treatment and weighed on an analytical balance after 24 h of conditioning in a darkened desiccator at a constant temperature (23–25 °C) and relative humidity (40–50%). Loaded filters were similarly conditioned and weighed for gravimetric determination of particle mass concentration. Afterwards, loaded filters were wrapped in solvent-rinsed aluminum foil and kept refrigerated until extraction and analysis.

Twenty-two PAHs were quantified on the collected samples: 1,2-dimethylnaphthalene (1,2 DM-Nap), 2,6-dimethyl-naphthalene (2,6 DM-Nap) acenaphthene (Ace), 2,3,5-trimethylnaphthalene (2,3,5-TM-Nap), acenaphthylene (Acy), anthracene (Ant), benzo[a]anthracene (B[a]A), benzo[a]pyrene (B[a]P) benzo[e]pyrene (B[e]P), benzo[b]fluoranthene (B[b]F), benzo[k]fluoranthene (B[k]F), benzo[g,h,i]perylene (B[ghi]Per), chrysene(Chry), dibenzo[a,h]anthracene (DBA), fluoranthene (Fla), fluorene (Flu), perylene (Per), indeno(1,2,3c,d)pyrene (IND), phenanthrene (Phe), pyrene (Pyr), 3,6-dimethylphenanthrene (3,6-dMePhe), 1-methylphenanthrene(1-MePhe). The sampling and analysis of the PAHs were performed according to ISO 12884 using a gas chromatograph (GC Agilent 5975C, Agilent, Santa Clara, CA, USA) coupled to a mass spectrometry detector (Agilent 7890A MS, Agilent, Santa Clara, CA, USA).

Briefly, the filter was extracted by Soxhlet with n-hexane for 24 h at a reflux rate of about 4 cycles per hour after the addition of an internal standard solution (d8-Nap, d10-A, d10-Phe, d10-Chr, d10-Pyr, d12-B[ghi]P, and d12-Perylene) to monitor recovery. Samples were concentrated by a rotary evaporator to 1 mL. Solid-phase extraction (SPE) cartridges were used as a pre-separation step before injection of the sample into the GC/MS. The SPE cartridges containing 2 g of silica were washed/conditioned with 10 mL of n-hexane. Then, the concentrated raw extract was loaded on top of the SPE cartridge and eluted with a mixture of n-hexane/dichloromethane (3:2). This eluted fraction was collected and finally concentrated in a pure N₂ stream. Each compound was quantified by GC/MS operating at an electron impact energy of 70 eV and using the selected ion monitoring (SIM) mode. A capillary column (30 m × 0.25 mm internal diameter × 0.25 μm film thickness) was used to quantify PAHs, and 1 mL of sample was injected in splitless mode. The GC conditions were as follows: 1.1 mL/min helium flow and a temperature–time program of 60–300 °C. The injector temperature was set to 285 °C, the transfer line to 280 °C, and the ion trap to 230 °C. Calibration curves were prepared with PAH concentrations between 0.05 and 10 ng in iso-octane. The NIST (1649b) certified reference material (CRM) was also used to ensure good accuracy and precision of PAH analysis. The expanded uncertainty (U_{exp}

k = 2) ranged from 6.3% to 23%, while the LOD of the method ranged from 0.6 pg/uL to 12.8 pg/uL (Supplementary Material, Table S1).

2.3. Data Analysis

The data collected from each sampling campaign were further analyzed using diagnostic PAH ratios (DRs) and PMF model. In addition, the concentrations of pollutants were used to estimate their potential health effects on humans and determine whether a substance, chemical or not, constitutes a potential risk to human health.

2.3.1. Diagnostic Ratios

The ratio values of individual PAH species in ambient air samples are commonly utilized as diagnostic tools to determine the origin of measured PAHs [25]. However, diagnostic ratios should be used with caution, as it can be challenging to distinguish between various sources, and they may be influenced by the reactivity of certain PAH species. The emission profile of PAHs from a specific source is influenced by the processes involved in their production [26]. For instance, low-temperature processes like wood burning typically result in the formation of low-molecular-weight PAHs, whereas high-temperature processes such as fuel combustion in engines tend to release higher-molecular-weight PAH compounds [27]. At elevated temperatures, organic compounds undergo cracking to form reactive radicals, which subsequently react to produce stable PAHs through pyrosynthesis. These PAHs exhibit lower levels of alkylation and contain more aromatic rings compared to petrogenic PAHs [28].

Diagnostic ratios of PAHs provide a means to differentiate between PAHs [29] and pyrolytic sources (e.g., fuel combustion), as well as various products of crude oil processing and biomass burning activities, such as bush, savanna, and grass fires, or coal [30]. Table 2 presents the diagnostic ratios commonly used in the literature for source identification, which were also used in the present study.

Table 2. Diagnostic ratios for PAHs source identification.

PAH Diagnostic Ratio	Indicator Source	Value Range	Reference
Ant/(Ant + Phe)	Petrogenic sources	<0.1	Fahr et al., 2022 [31]
	Pyrogenic sources	>0.1	
IND/(IND + B[ghi]P)	Petrogenic sources	<0.2	G.O. Duodu et al., 2017 [32] Marek & Jasec, 2012 [29]
	Combustion of liquid fuels	0.2–0.50	
Fluo/(Fluo + Pyr)	Grass, wood, and coal combustion	>0.5	Yunker et al., 2002 [30] Ravindra et al., 2008a [25]
	Gasoline	<0.5	
B[a]P/(B[a]P + Chry)	Diesel	>0.5	Ravindra et al., 2008a [25]
	Petrogenic sources	<0.2	
B[b]Fl / B[k]Fl	Mixed (petrogenic/pyrogenic)	0.2–0.50	Inam et al., 2016 [33]
	Pyrogenic sources	>0.5	
Flua/(Flua + Pyr)	Diesel	>0.5	Ravindra et al., 2008a [25]
	Petrogenic sources	<0.4	
	Liquid fossil fuel burning	0.4–0.5	
B[a]P/B[ghi]P	Coal, wood, and grass burning	>0.5	Fahr et al., 2022 [31]; Marek & Jasec, 2012 [29]
	Non-traffic emissions	<0.6	
IND/B[ghi]P	Traffic emissions	>0.6	Marek & Jasec, 2012 [29]; Fiore et al., 2021 [34]
	Gasoline	<0.4	
Pyr/B[a]P	Diesel	~1	Ravindra et al., 2008 [25]
	Gasoline	~1	
B[a]A/ (B[a]A + Chry)	Diesel	~10	Ravindra et al., 2008 [25]
	Petrogenic sources	<0.2	
	Petroleum and fuel oil combustion	0.2–0.35	
	Coal, wood, and grass combustion	>0.35	Fiore et al., 2021 [34]; Fahr et al., 2022 [31]

Table 2. Cont.

PAH Diagnostic Ratio	Indicator Source	Value Range	Reference
Flua/Pyr	Petrogenic sources	<1	G.O. Duodu et al., 2017 [32]
$\Sigma\text{COMP}/\Sigma\text{16PAHs}$	Combustion of solid fuel	>1	
	Combustion	~1	Fahr et al., 2022 [31]
$\text{B[a]P}/\text{B[a]P} + \text{B[e]P}$	Fresh particles	~0.5	Marek & Jasec, 2012 [29]
	Photolysis	<0.5	
LMW/HMW	Pyrogenic sources (coal, grass, and burning of wood)	<1.0	Fahr et al., 2022 [31]; Marek & Jasec, 2012 [29]
	Petrogenic sources (fuel or one refined petroleum product)	>1.0	
Phe/Ant	Combustion of solid fuel	<10	G.O. Duodu et al., 2017 [32]
	Petrogenic	>10	
Total Index [Flua/(Flua + Pyr), Ant/(Ant + Phe), B[a]A/(B[a]A + Chry), IND/(IND + B[ghi]P)]	Low-temperature source (petroleum)	<4	Bootdee et al., 2016 [35]
	High-temperature source (combustion)	>4	
$\text{C11A7}/\Sigma\text{11A7}$	Combustion	~1	Ravindra et al., 2008 [25]

Additionally, the total index, as described by Bootdee et al., 2016 [35], was used to confirm emission and identify the profile of PAHs (Supplementary Equation (S1)).

2.3.2. Positive Matrix Factorization (PMF) Model

Receptor models are widely used to analyze and reconstruct the contributions of various emission sources of atmospheric pollutants, such as particulate matter. This reconstruction is based on ambient measurement data, specifically the chemical composition of particulate matter, obtained from monitoring sites (i.e., receptors). The receptor model used in this study was the positive matrix factorization (PMF). It incorporates a weighting system that considers the errors associated with data points, by using them as individual weights. This approach also adjusts error estimates to accommodate missing data and points below the detection limit [36]. Additionally, non-negative constraints are applied to ensure the derivation of factors that are more aligned with physical interpretations. In this study, the USEPA PMF version 5.0 was used, which offers three advanced tools to evaluate the rotational ambiguity and investigate the uncertainty of the derived solution: bootstrap (BS) analysis, the displacement (DISP) method, and a combination of DISP and BS (BS–DISP), as well as the possibility to apply constraints to the solution. These additional features were used in the present study for assessing and improving the solution.

2.3.3. Data Pretreatment, Model Runs, and Evaluation of PMF Solutions

PMFv.5 model was run for each sampling site, with datasets consisting of $n = 45$ and $n = 90$ samples for the Municipality of Peloponnese and Aristotelous sites, respectively (i.e., datasets with sufficient data for the model's application). For the model input matrix, low-molecular-weight PAHs were excluded due to their volatility [37]. Therefore, the sum of the high-molecular-weight PAHs (i.e., benzo[b]fluoranthene, benzo[k]fluoranthene, benzo[e]pyrene, benzo[a]pyrene, indeno[1,2,3-cd]pyrene and benzo[ghi]perylene) was considered as one species, "SPAHS". To avoid double mass counting of certain species, where applicable, either the ion or the elemental form of these species was included in the analysis (e.g., Ca and Ca^{2+}), depending on their uncertainty and impact on the model's solution. "Bad" species were excluded from the analysis due to a high percentage of missing values or very low signal/noise ratio (<0.2). Furthermore, depending on the case, some species were set as "weak" due to their low signal/noise ratio ($0.2 < S/N < 2$) and/or poor scaled residuals (d-matrix). Finally, outliers were excluded from the analysis. Data below the detection limit (with the maximum reported detection limit was used as a conservative limit for all samples) were substituted with one-half of the detection limit, and missing concentration data were substituted with the median value [38]. The additional modeling uncertainty was adjusted to 8–12%.

A range of solutions was examined with different numbers of factors (3–8) in each case. Thirty runs were executed for each scenario. The robustness of the solutions was assessed according to the recommendations of the European guide on air pollution source apportionment with receptor models [39].

PMFv.5 provides three advanced tools to evaluate the rotational ambiguity of the derived PMF solution: bootstrap (BS) analysis, the displacement (DISP) method, and a combination of DISP and BS (BS–DISP). BS estimates the effect that random errors in the matrix/dataset have on the solution; DISP explicitly explores the rotational ambiguity, and BS–DISP is a combination of both [22]. In the present study, BS, DISP, and BS–DISP runs were conducted to evaluating the model’s solutions. Specifically, 100 bootstrap runs were executed for each dataset (with the default minimum correlation $r^2 = 0.6$), and the results were considered reliable if >80% of the factors were mapped. DISP runs resulted in the validity of the final PMF solutions, as no factor swaps (i.e., exchanges) were observed for the smallest $dQ_{max} = 4$ while the decrement of Q was <1%. Through BS–DISP analysis, the final solution was considered to be valid according to [40]. A good correlation was noticed between the model-predicted and the measured PM_{10} mass concentration ($r^2 > 0.8$) in all cases. In the following, the results from PMF application for the Municipality of Peloponnese and Aristotelous are presented.

2.4. Carcinogenic Lifetime Risk Assessment

Assessing whether a substance, whether chemical or not, poses a potential risk to human health comprises a multifaceted procedure. Dose–response assessment entails examining the relationship between exposure to a substance and the occurrence of adverse health effects among those exposed. The probability of developing cancer over a lifetime for people living in selected areas was estimated based on the study by M.M. Jackson (2005) [41]. In quantitative carcinogenic risk assessment, the dose–response correlation is expressed in terms of a potency slope, which is used to calculate the probability of carcinogenic risk associated with an estimated exposure (95th percentile upper confidence limit of the slope of the dose–response curve) [42]. The cancer risk (CR) values of 10^{-6} – 10^{-4} are categorized as negligible risk, potential risk, and serious high cancer risks, with values bellow $<10^{-6}$ considered acceptable, and 10^{-6} regarded as the most tolerable risk [17,43,44]. Finally, the cancer risk for each pollutant was aggregated to calculate the total cancer risk, and then the overall cancer risk was expressed as “chances per million”:

$$(\text{Total Cancer Risk}) (1 \times 10^6) = \text{Total Cancer Risk in chances per million}$$

Different hypothetical scenarios of human exposure were selected for application to the population. Specifically, the following cases were considered:

- The case of a male and a female living and working at the place of exposure, i.e., 24 h/day.
- The case of a male and a female living at the place of exposure (their place of residence) for 14 h/day, and working outside of that region.
- The cases of a child in the age groups of 0–2 and 2–16 years old, living at the place of exposure, i.e., 24 h/day.

The exposure period was selected to be 350 days/year in all cases. Furthermore, specific values for the parameters IR (inhalation rate) and BW (body weight) were chosen according to the literature [43,45] for the residents. Specifically:

- For males: IR = 16.4 (m^3 /day) and BW = 76 (kg);
- For females: IR = 12.6 (m^3 /day) and BW = 63 (kg);
- For children of age 2–16 years old: IR = 10.8 (m^3 /day) and BW = 32.5 (kg);
- For children of age 0–2 years old: IR = 4.9 (m^3 /day) and BW = 10.3 (kg).

2.5. Approach Used for the Estimation of Potential Cancer Risk

In the study by M.M. Jackson (2005) [41], the contribution of road traffic to air pollution levels in Dar-es-Salaam, Tanzania, was examined, and a risk assessment was conducted for people in the nearby area. In the present study, the same methodology was used to estimate the potential cancer risk for residents in the region due to various of pollutants, considered as potentially carcinogenic substances. The cancer risk (R) was calculated using Equations (1) and (2):

$$CDI = \frac{CA \times IR \times ED \times EF \times L}{BW \times AT \times 365} \quad (1)$$

$$R = CDI \times P \quad (2)$$

where P is the cancer potency for the pollutants ($\text{mg} \cdot \text{kg}^{-1} \cdot \text{day}^{-1}$)⁻¹ that were selected according to US-EPA Regional Screening Level (RSL) Summary Supplementary 2019 [46]. The CDI (chronic daily intake) dose ($\text{mg} \cdot \text{kg}^{-1} \cdot \text{day}^{-1}$) was calculated from Equation (1), with CA: the concentration of pollutant in the air (mg/m^3), IR: the inhalation rate (m^3/h), EF: the exposure frequency (days/year), ED: the exposure duration per day (h/day), L: the length of the exposure (years), BW: the average body weight (kg), and AT: the averaging time of 80 years length for carcinogens [43].

The potential risk and characterization of a complex PAH mixture can also be identified using the equivalent toxicity concentration (TEQ), as described by Bootdee et al., 2016 [35]. This parameter is calculated by summing the concentrations of individual PAHs, each multiplied by its toxic equivalent factor (TEF) relative to the carcinogenic potency of BaP (Equation (3)), which is used as a reference carcinogenic compound. According to recent knowledge, BaP is responsible for approximately 50% of the carcinogenic potential of PAHs, and this scientific background is considered sufficient for establishing a limit value. The toxicity equivalent concentration (TEQ) was calculated based on the work of Nisbet and LaGoy (1992) [47], who provided a set of TEFs that more accurately reflects the current understanding of the relative potencies of the different PAHs. BaP and DBA are defined as the most carcinogenic components, with TEF equal to 1.0, while noncarcinogenic PAHs have TEF equal to 0. The European Union sets the limit value for equivalent toxicity concentration at $1 \text{ ng}/\text{m}^3$.

$$\begin{aligned} \text{TEQ} = & 0.001(\text{NAP} + \text{ACY} + \text{ACE} + \text{FLUO} + \text{PHE} + \text{FLUA} + \text{PYR}) \\ & + 0.01(\text{ANT} + \text{BeP} + \text{CHR}) \\ & + 0.1(\text{BaA} + \text{BbF} + \text{BkF} + \text{IND}) + \text{BaP} + \text{DBA} \end{aligned} \quad (3)$$

Furthermore, the mutagenic equivalent concentration (MEQ) can be used for assessments associated with adverse health effects (e.g., pulmonary diseases) but not for assessing cancer risk. The MEQ was determined by multiplying the concentration of each PAH compound by the mutagenic equivalent factor (MEF) relative to the mutagenic potency of BaP (Equation (4)).

$$\begin{aligned} \text{MEQ} = & 0.082(\text{BaA}) + 0.017(\text{CHR}) + 0.25(\text{BbF}) + 0.11(\text{BkF}) \\ & + 0.31(\text{IND}) + 0.29(\text{DbA}) + 0.19(\text{BPER}) + \text{BaP} \end{aligned} \quad (4)$$

The inhalation cancer risk (ICR) was determined to estimate the value of the cancer risk from PAHs exposure, according to the following equation (Equation (5)).

$$\text{ICR} = \text{TEQ} \times \text{IUR}_{\text{BaP}} \quad (5)$$

where IUR_{BaP} , or the inhalation unit risk, represents the probability of the maximum theoretical limit of the number of people with cancer in the respiratory system caused by inhalation at an equivalent concentration of $1 \text{ } \mu\text{g}/\text{m}^3$ BaP over a lifetime of 70 years. Two different IUR_{BaP} values were selected for the inhalation cancer risk assessment, 1.10×10^{-6} per m^3/ng , according to the California Environmental Protection Agency (CalEPA), and 8.70×10^{-5} per m^3/ng , according to the World Health Organization [48,49].

3. Results and Discussion

3.1. PAH Concentration Levels

Statistics of individual and total PAH concentrations for the winter and summer campaigns at each area are presented in the Supplementary Material (Tables S2–S4). For the Municipality of Peloponnese, the highest total PAH concentrations (Σ_{22} PAHs) during the winter campaign were observed at station S1 (11.45 ng/m³), followed by those at station S2 (9.84 ng/m³) and station S3 (8.84 ng/m³). PAHs derived from combustion (COMPAHs) were detected at concentrations equal to 11.95, 11.11, and 9.01 ng/m³, at S1, S2, and S3, respectively. In all three stations, high values of concentrations were observed for six compounds classified as potential carcinogenic to humans (CANPAHs): BaA (benz(a)anthracene), BbF (benzo(b)fluoranthene), BkF (benzo(k)fluoranthene), IcdP (indeno(1,2,3-c,d)pyrene), Chry (chrysene), and the well-known carcinogen BaP (benzo(a)pyrene). For the winter period, BaP was detected at concentrations of 1.28 ng/m³, 1.26 ng/m³, and 1.13 ng/m³ at S1, S3, and S2, exceeding the threshold of 1 ng/m³ (EU Directive 2004/107 /EC). During the summer period, much lower (compared to the winter period) concentrations of total PAHs (Σ_{22} PAHs) were observed as olive pomace industries were out of operation. The concentrations at sites S1, S2, and S3 were 0.99, 1.20, and 0.70 ng/m³, respectively. Σ COMPAHs average values were 0.70, 0.78, and 0.52 ng/m³ at S1, S2, and S3, respectively. It must be pointed out that CANPAHs were absent at all sampling sites during the summer campaign, except for Chry, which was detected at low concentrations only at sites S1 and S2. The compositional pattern of PAHs by total rings calculated from all the data at the three sites of Peloponnese (S1, S2, and S3) for winter period is shown in Figure 5.

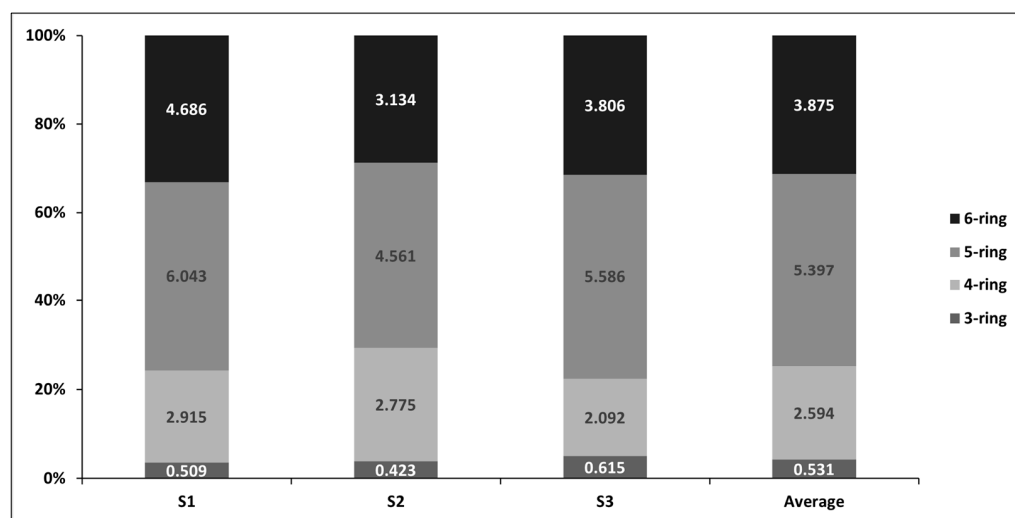


Figure 5. Composition pattern of total PAHs (ng/m³) in areas of Peloponnese in winter period.

As observed in Figure 5, high-molecular-weight PAHs (five and six rings) are the most abundant, averaging ~75% of total PAHs across the three areas. The four-ring PAHs averaged accounted for approximately 20%. The three-ring PAHs percentages were lower, i.e., at 3.60%, 3.88%, and 5.08%, respectively, for the three areas (S1, S2, and S3), respectively. In contrast, a noticeable seasonal difference was observed in the composition of PAHs during the summer campaign, with most PAHs concentrations being below the detection limit. Specifically, only PAHs with three and four rings were observed during the summer period, and the difference between seasons is evident in Figure 6. The average concentration from the three sites was calculated to be nine times higher during winter, with total averaged concentration from three sites to be 12.1 and 1.34 ng/m³ for winter and summer, respectively.

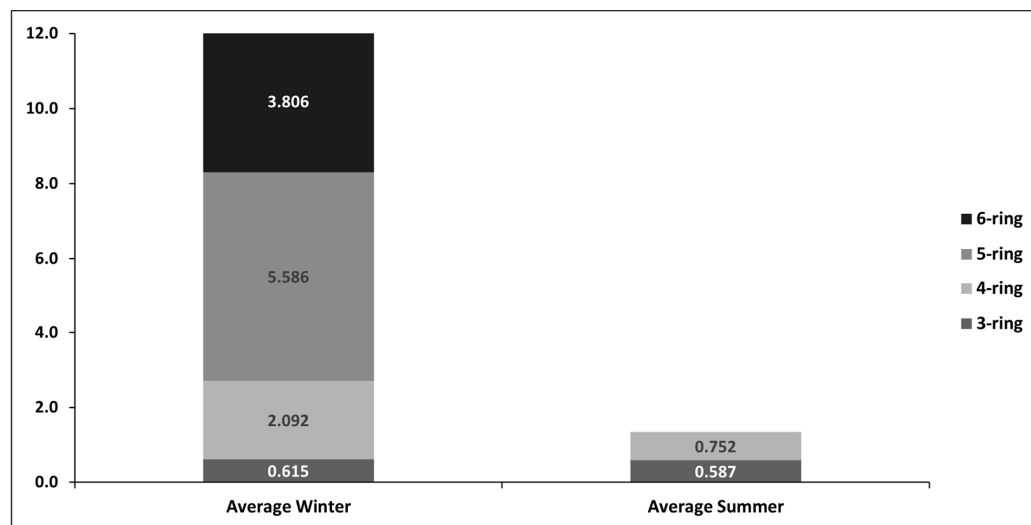


Figure 6. Seasonal differential of composition pattern of total PAHs (ng/m^3) in areas of Peloponnese.

Numerous studies have investigated the concentration levels of PAHs in areas around olive pomace oils [25,50,51]. However, the footprint of olive pomace industries on air quality remains unknown. The study by Leon-Camacho et al., 2003 [52] mentions that the “two stage” pomace has a humidity of around 70% and contains numerous chemical compounds, such as metals, both alkaline and alkaline-earths, sugars, and polyphenols. Due to the harsh conditions of the drying process, unusually high amounts of PAHs have been detected in crude olive pomace oil (400–200 ppb of BaP). In another study, a high number of PAHs with a wide range of molecular weights in very high concentrations were detected in olive pomace oils [53]. Therefore, the potential for significant PAH emissions during the harsh conditions of the pomace drying process (except for olive pomace oils) should be further investigated.

Regarding PAH’s concentrations at Oinofyta (all sites), the total PAHs ($\Sigma_{22}\text{PAHs}$) average levels were A1: $2.17 \text{ ng}/\text{m}^3$, A2: $0.93 \text{ ng}/\text{m}^3$, A3: $1.08 \text{ ng}/\text{m}^3$, and A4: $0.75 \text{ ng}/\text{m}^3$. The average $\Sigma\text{COMPAHs}$ level of A1 and A4 was, on average, $0.39 \text{ ng}/\text{m}^3$, while the average level of A2 and A3 was $0.50 \text{ ng}/\text{m}^3$. $\Sigma\text{CANPAHs}$ were detected at very low concentration levels. The well-known carcinogen benzo(a)pyrene had average levels of 0.03, 0.05, 0.04, and $0.04 \text{ ng}/\text{m}^3$ at A1, A2, A3, and A4, respectively. Although industries with diverse activities exist within the broader area, low concentrations of total PAHs were observed. This can be attributed to the sampling period, i.e., September to October, during which contribution to combustion from residential heating or winter starting of vehicles’ engines are almost absent [26]. For comparison, a study by [54] conducted in the industrial area of Elefsina, Greece, between November 2001 and June 2002 found significantly higher total PAHs ($\Sigma_{13}\text{PAHs}$) at $7.93 \text{ ng}/\text{m}^3$, while the known carcinogen B(a)P had an average value equal to $0.71 \text{ ng}/\text{m}^3$. Also, higher total PAH values were found in the industrial region of Taichung, central Taiwan [55], during the summer period, where total PAHs ($\Sigma_{22}\text{PAHs}$) were 13.24 and $13.55 \text{ ng}/\text{m}^3$, respectively.

At the urban/traffic center of Aristotelous during the winter campaign, the total PAHs ($\Sigma_{22}\text{PAHs}$) concentration was $6.30 \text{ ng}/\text{m}^3$. $\Sigma\text{COMPAHs}$ was $5.87 \text{ ng}/\text{m}^3$ and CANPAHs was $3.89 \text{ ng}/\text{m}^3$, while the average value of B(a)P was $0.51 \text{ ng}/\text{m}^3$. Considering the data collected during the summer campaign, a total PAH value of $5.84 \text{ ng}/\text{m}^3$ was observed. A significant increase in the concentrations of acenaphthene, fluorene, and especially phenanthrene was measured during the period between 13 July and 20 July 2016. The total concentration of COMPAHs was $1.09 \text{ ng}/\text{m}^3$. The total value of CANPAHs was detected at $0.52 \text{ ng}/\text{m}^3$, while the average value of B(a)P was $0.08 \text{ ng}/\text{m}^3$. The concentrations observed at Aristotelous are higher compared to those reported from a previous study conducted at

the center of Athens [56]; however, they are in the lowest range of reported values for other Greek and European urban locations [26].

As far as the concentration of the most well-known carcinogen, BaP, is concerned, much lower values were recorded in the present study, compared to those measured at individual sites in three other large European cities: 1.8 ng/m³ (over one year) in central Genoa at a busy and “canyon” street [57], 1.9 ng/m³ (over 19 months) in central London at a street with moderate traffic [58], and 4.4 ng/m³ (during winter months) at a busy street in Copenhagen [59]. An indicative comparison with the annual limit value (1 ng/m³) showed exceedances in all three sites in the area of Peloponnese. In the following table (Table 3), the statistics of PAHs for the winter campaign in the Municipality of Peloponnese are presented.

Table 3. Statistics of PAHs concentrations (ng/m³) adsorbed to ambient PM₁₀ (ng/m³) for winter campaign in Municipality of Peloponnese (N.D. = not detected).

	S1 (Meligalas, <i>n</i> = 10)			S2 (Skala, <i>n</i> = 10)			S3 (Messini, <i>n</i> = 10)		
	Mean	Min–Max	Stdev	Mean	Min–Max	Stdev	Mean	Min–Max	Stdev
Acenaphthylene	0.022	0.016–0.028	0.006	0.029	0.003–0.092	0.032	0.032	0.017–0.045	0.013
1,2-dimethylnaphthalene	0.022	0.007–0.040	0.011	0.020	0.004–0.047	0.016	0.027	0.001–0.053	0.016
2,6-dimethylnaphthalene	0.012	0.005–0.021	0.005	0.012	0.003–0.021	0.007	0.016	0.007–0.050	0.013
Acenaphthene	0.111	0.032–0.255	0.074	0.104	0.008–0.200	0.070	0.104	0.027–0.155	0.048
2,3,5-trimethylnaphthalene	0.021	0.015–0.028	0.004	0.021	0.003–0.030	0.008	0.030	0.016–0.085	0.021
Fluorene	0.128	0.000–0.440	0.179	0.088	0.018–0.181	0.059	0.139	0.019–0.294	0.097
Phenanthrene	0.248	0.034–0.755	0.247	0.193	0.040–0.304	0.115	0.260	0.016–0.500	0.161
1-methylphenanthrene	N.D.	N.D.	N.D.	0.012	0.012–0.012	N.D.	0.112	0.087–0.136	0.035
3,6-dimethyl phenanthrene	N.D.	N.D.	N.D.	0.011	0.010–0.011	0.001	0.100	0.100–0.100	N.D.
Anthracene	N.D.	N.D.	N.D.	0.009	0.009–0.009	N.D.	0.080	0.069–0.090	0.015
Fluoranthene	0.238	0.094–0.679	0.211	0.218	0.020–0.652	0.205	0.181	0.083–0.430	0.115
Pyrene	0.317	0.089–0.936	0.297	0.276	0.029–0.968	0.295	0.239	0.122–0.518	0.153
benz(a)anthracene	0.800	0.306–1.701	0.619	0.880	0.255–2.047	0.736	0.518	0.185–1.051	0.391
Chrysene	1.560	0.210–3.306	1.120	1.401	0.164–3.065	1.100	1.154	0.170–2.674	1.013
benzo(b)fluoranthene	3.238	0.176–12.19	3.795	2.273	0.054–8.159	2.679	3.112	0.215–9.960	4.001
benzo(k)fluoranthene	1.146	0.214–2.588	0.804	0.813	0.022–1.782	0.693	0.857	0.077–2.069	0.849
benzo(e)pyrene	1.994	0.357–5.222	1.627	1.242	0.049–3.556	1.148	1.627	0.185–4.625	2.007
benzo(a)pyrene	1.277	0.121–3.987	1.415	1.126	0.016–2.689	1.081	1.263	0.277–1.818	0.857
perylene	0.382	0.175–0.691	0.220	0.349	0.204–0.489	0.147	0.354	0.335–0.373	0.027
indeno(1,2,3-c,d)pyrene	2.404	0.392–6.659	2.102	1.549	0.048–4.696	1.568	2.007	0.157–6.591	2.519
dibenzo(a,h)anthracene	0.339	0.119–0.758	0.290	0.247	0.089–0.499	0.168	0.392	0.104–0.622	0.263
benzo(ghi)perylene	1.943	0.158–5.026	1.591	1.338	0.088–3.886	1.225	1.407	0.177–4.759	1.689
ΣPAHs	11.45	0.210–45.60	13.27	9.839	0.445–30.78	10.11	8.836	0.424–33.82	11.77
ΣCANPAHs	8.396	0.176–31.48	9.356	6.509	0.141–20.87	7.312	7.218	0.334–22.91	8.848
ΣCOMPAHs	11.95	0.176–42.59	12.64	11.11	0.327–29.44	9.749	9.014	0.083–32.62	11.82
PM ₁₀	36.34	7.106–186.0	20.17	43.89	14.02–178.0	18.31	36.05	6.129–336.7	39.18

3.2. Comparison and Seasonal Variation

Comparing the results from the two sampling campaigns at the Municipality of Peloponnese, the total concentration of PAHs ($\Sigma 22\text{PAHs}$) in the winter campaign was increased by 91%, 83%, and 92% at sites S1, S2, and S3, respectively. In the Aristotelous area, significant seasonal variation was recorded, with summer levels prevailing by 40% compared to winter due to high concentrations in the last days of sampling. The lowest PAH levels were observed in the industrialized area of Oinofyta, which were similar to those in the Municipality of Peloponnese during the summer campaign.

Among all the analyzed compounds, B[b]F was the most abundant, constituting approximately 20% of the total concentration of PAHs during the winter campaign at the Municipality of Peloponnese. Meanwhile, B[ghi]P dominated, comprising approximately 19% of the total concentration of PAHs at Aristotelous (Figures 7 and 8). These findings align closely with a previous study in the same area, highlighting the significant contribution of vehicular emissions [54]. In summer, at the Municipality of Peloponnese, only the low-molecular-weight compounds prevailed, while in Aristotelous, phenanthrene, fluorene, and acenaphthene were the most abundant in high concentrations, likely from local sources, transported pollutants, or both (Figure 9). Previous studies have reported that the pollution status of an area is often considered a mixed signature of both local and external sources [60]. In the Oinofyta area, phenanthrene and benzo(ghi)perylene (indicators of vehicle emission indicators) prevailed. The significant reduction in PAHs during the summer period in Peloponnese, where the olive oil agricultural activities had ended, clearly indicates the impact of olive pomace oil industries on local air quality during the winter period.

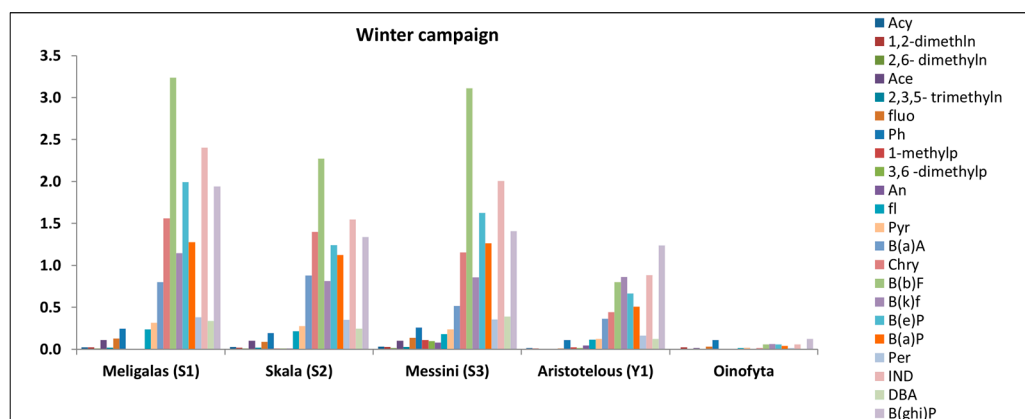


Figure 7. Spatial winter differentiation of the average concentrations of PAHs (ng/m^3) in all study areas.

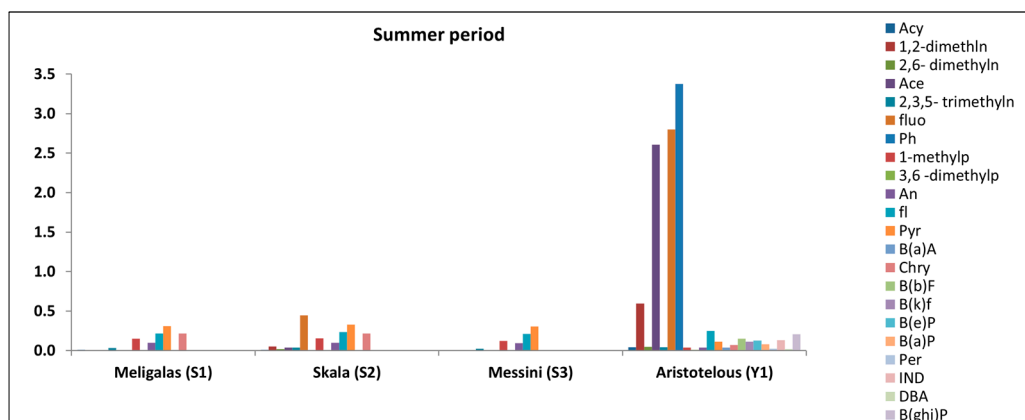


Figure 8. Spatial summer differentiation of the average concentrations of PAHs (ng/m^3) in all study areas.

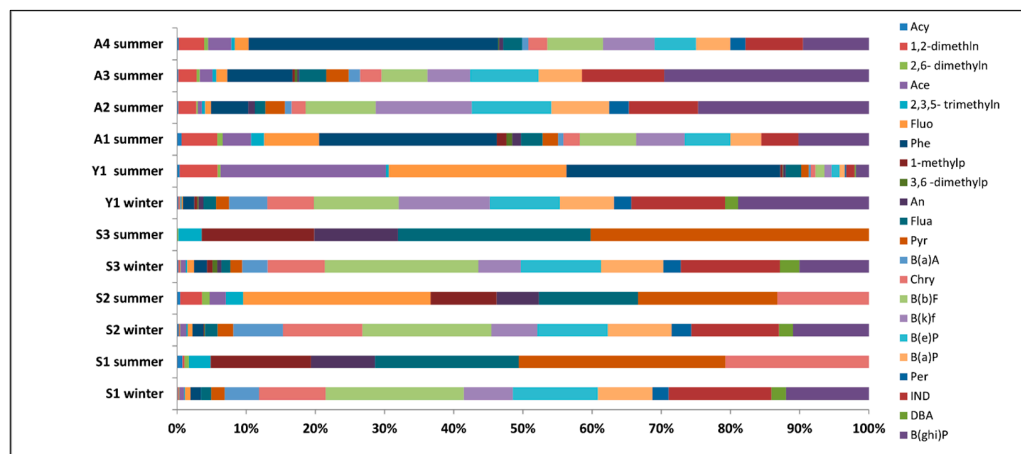


Figure 9. Spatial and seasonal differentiation of the average individual contribution (%) of PAHs in all study areas.

The average concentrations of the well-known carcinogen B(a)P during the winter campaign were observed to be higher in the areas of the Municipality of Peloponnese (Meligalas: 1.28 ng/m³, Skala: 1.13 ng/m³, Messini: 1.26 ng/m³) compared to the corresponding average value in the area of Aristotelous (0.51 ng/m³). In the summer, B(a)P was below the detection limit in the areas of the Municipality of Peloponnese, while concentrations were similar among other sampling sites: 0.08 ng/m³ in Aristotelous, and 0.03 ng/m³, 0.05 ng/m³, 0.04 ng/m³, and 0.04 ng/m³ in A1, A2, A3, and A4 sites in Oinofyta area, respectively (Figure 10b). In addition, Figure 10a confirms the seasonal variation in both the Municipality of Peloponnese and Aristotelous.

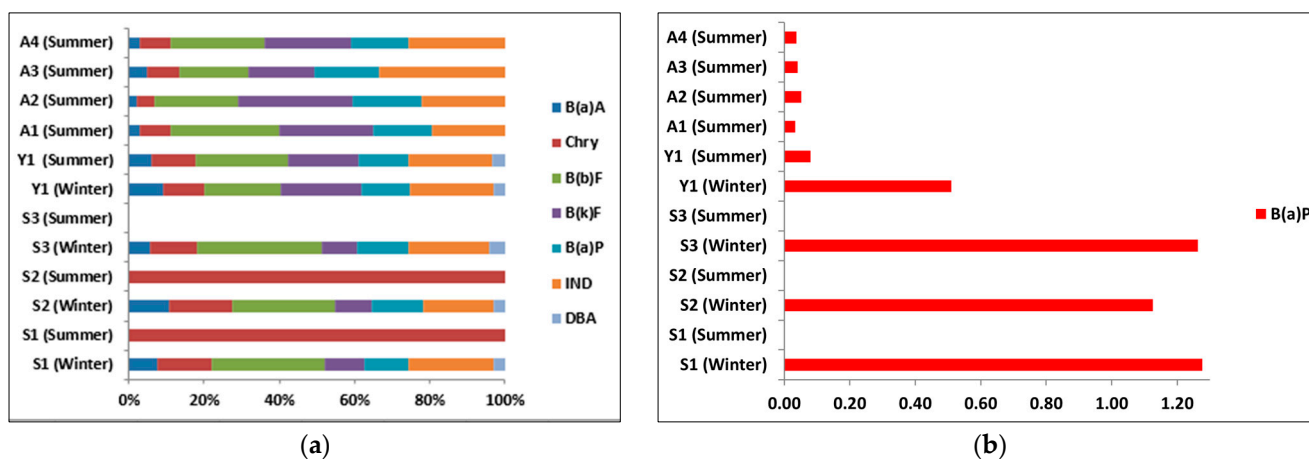


Figure 10. Spatial and seasonal variation of (a) the average individual contribution (%) of CANPAHs and (b) the average concentration of BaP (ng/m³), in all study areas.

During the winter campaign, ΣCOMPAHs presented an approximately 53% increase in the areas of the Municipality of Peloponnese compared to the area of Aristotelous, likely due to increased emissions from residential heating in the area (i.e., mainly biomass combustion). Additionally, the operation of olive pomace industries in this area possibly contributes to the increased levels. In the area of Oinofyta, ΣCOMPAHs were approximately 28% compared to ΣPAHs, likely due to the high contributions from the national highway and the industries in the area.

Furthermore, significant seasonality for ambient PAH levels has been reported by several investigators [54]. Generally, PAH levels tend to decrease during the summer, reflecting changes in prevailing meteorological conditions such as higher temperature inversions and increased photocatalytic and thermal decomposition of PAHs during the

summer campaign. Additionally, selective emissions are more prevalent during the winter season. This situation was also observed in our study across all three areas of interest.

3.3. Health Risk Assessment

The potential health effects were estimated, using the methodologies described in the previous paragraphs, for all the pollutants as a complex mixture (TEQ, MEQ, ICR; Table 4). Assessments for each pollutant were conducted for different hypothetical scenarios of human exposure (duration of the exposure, age), regarding their exposure intake (CDI) and then cumulatively, to estimate the total lifetime cancer risk (R) for the residents of all study areas (Table 5).

Table 4. TEQ and MEQ concentrations (mean ± SD) and ICR of PAHs of sites for both seasons.

Sampling Sites/ Risk Assessment Variables	Saverage Winter	Saverage Summer	Aaverage Winter	Y1 Winter	Y1 Summer	
TEQ concentration (ng/m ³)	2.23 ± 0.20 (n = 3)	4.15 × 10 ⁻³ ± 1.20 × 10 ⁻³ , (n = 3)	0.05 ± 0.03 (n = 4)	0.92 ± 0.90 (n = 36)	0.11 ± 0.11 (n = 36)	
MEQ concentration (ng/m ³)	3.13 ± 0.34 (n = 3)	3.67 × 10 ⁻³ ± 1.73 × 10 ⁻³ , (n = 3)	0.09 ± 0.06 (n = 4)	1.38 ± 1.21 (n = 36)	0.18 ± 0.17 (n = 36)	
ICR	WHO (8.7 × 10 ⁻⁵ m ³ /ng)	1.94 × 10 ⁻⁴	2.70 × 10 ⁻⁷	4.50 × 10 ⁻⁶	7.97 × 10 ⁻⁵	9.71 × 10 ⁻⁶
	CalEPA (1.1 × 10 ⁻⁶ m ³ /ng)	2.46 × 10 ⁻⁶	3.41 × 10 ⁻⁹	1.01 × 10 ⁻⁶	1.01 × 10 ⁻⁶	1.23 × 10 ⁻⁷
Risk (ICR × 10 ⁶)	WHO	194.2	0.3	4.5	79.7	9.7
	CalEPA	2.5	3.4 × 10 ⁻³	1.0	1.0	0.1

Table 5. Lifetime cancer risk (adults, 80 years) of PAHs in composite of sites for both seasons.

Sampling Sites/ Pollutants	Saverage Winter	Saverage Summer	Aaverage Winter	Y1 Winter	Y1 Summer
BaP	0.28	N.D.	0.01	0.12	0.02
BaA	0.02	N.D.	1.50 × 10 ⁻⁴	0.01	8.11 × 10 ⁻⁴
BbF	0.06	N.D.	1.37 × 10 ⁻³	0.02	3.45 × 10 ⁻³
BkF	2.18 × 10 ⁻³	N.D.	1.46 × 10 ⁻⁴	2.00 × 10 ⁻³	2.60 × 10 ⁻⁴
CHRY	3.18 × 10 ⁻⁴	1.94 × 10 ⁻⁵	3.75 × 10 ⁻⁶	1.02 × 10 ⁻⁴	1.62 × 10 ⁻⁵
DBahA	0.08	N.D.	N.D.	0.03	4.87 × 10 ⁻³
I123cdP	0.05	N.D.	1.35 × 10 ⁻³	0.02	3.06 × 10 ⁻³
1Methyl	2.78 × 10 ⁻⁴	6.27 × 10 ⁻⁴	5.59 × 10 ⁻⁵	1.76 × 10 ⁻⁴	2.42 × 10 ⁻⁴
Ace	1.48 × 10 ⁻³	N.D.	2.29 × 10 ⁻⁴	7.77 × 10 ⁻⁵	0.04
Fluo	1.10 × 10 ⁻³	N.D.	3.22 × 10 ⁻⁴	1.18 × 10 ⁻⁴	0.03
Ant	3.09 × 10 ⁻³	3.71 × 10 ⁻⁴	4.10 × 10 ⁻⁴	3.24 × 10 ⁻³	2.71 × 10 ⁻³
Flua	1.97 × 10 ⁻³	1.38 × 10 ⁻³	1.59 × 10 ⁻⁴	1.08 × 10 ⁻³	2.32 × 10 ⁻³
Pyr	1.93 × 10 ⁻³	8.34 × 10 ⁻⁵	9.86 × 10 ⁻⁴	8.62 × 10 ⁻⁴	7.79 × 10 ⁻⁴
Σ	0.50	2.48 × 10 ⁻³	0.01	0.20	0.10

3.3.1. TEQ, MEQ, and Inhalation Cancer Risk Assessment

Due to minor differences observed among the concentrations measured at sites within the Municipality of Peloponnese (S1, S2, and S3) and in the area of Oinofyta (A1, A2, A3, and A4), the concentrations were merged into averaged values, denoted as S_{average} and A_{average}, respectively, to provide representative assessments across the study areas. As a result, this approach ensures a comprehensive analysis while accounting for variations among individual sites.

For the Municipality of Peloponnese, during the winter campaign, the average value of equivalent toxicity concentration (TEQ) was calculated to be equal to 2.41, 1.95, and 2.33 ng/m³ at sites S1, S2, and S3, respectively, with overall average TEQ concentration of

2.23 ng/m³ ($S_{average}$). Specifically, BaP contributed for 53%, 58%, and 54% of the carcinogenic activity of TEQ at sites S1, S2, and S3, respectively. During the summer campaign, TEQ was detected in low concentrations: 0.004, 0.004, and 0.001 ng/m³ at S1, S2, and S3, respectively, with overall average TEQ concentration equal to 4.15×10^{-3} ng/m³ ($S_{average}$). Given these considerations, during the winter period, the values of TEQ and MEQ were higher due to elevated concentrations of PAHs. On the contrary, during the summer period, they were nearly negligible due to significantly reduced PAH concentrations (Figure 11).

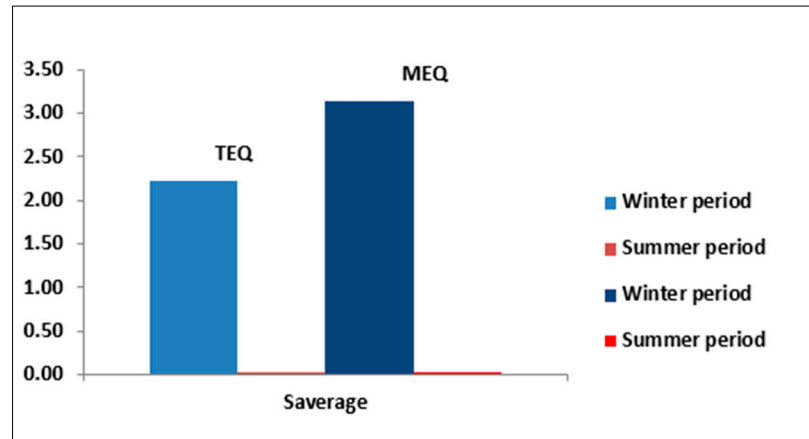


Figure 11. Seasonal variation of TEQ and MEQ (ng/m³) in the Municipality of Peloponnese.

The average values of TEQ and MEQ for Aristotelous were estimated to be 0.92 and 1.38 ng/m³, respectively, for the winter campaign, and 0.11 and 0.18 for the summer campaign. With regard to these observations, there is obvious seasonal variation, which is attributed to the significant differences in the concentrations of measured PAHs (Figure 12).

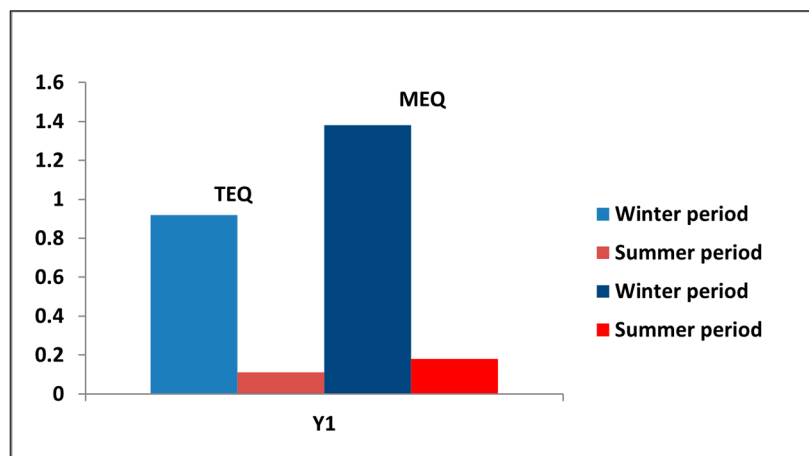


Figure 12. Seasonal differentiation of TEQ and MEQ (ng/m³) of Aristotelous.

The ICR average values during the winter period were estimated to be 79.7×10^{-6} and 1.01×10^{-6} according to WHO and CalEPA, respectively. For the summer campaign, ICR average values were calculated to be 9.71×10^{-6} and 1.23×10^{-7} . Therefore, for both seasons, the number of cancer cases per million people were within the ICR range of potential health risk (10^{-6} – 10^{-4}), indicating 79.7 and 1 cases of cancer per million people for the winter period, according to WHO and CalEPA, respectively. Furthermore, for the summer period, the inhalation cancer risk was lower, with an estimated 9.7 cancer cases according to WHO, which were within the ICR range of potential health risk (10^{-6} – 10^{-4}). In addition, the estimated cancer cases per million people were 0.1 according to CalEPA, indicating a lower-bound zero risk during the same period (Figure 13).

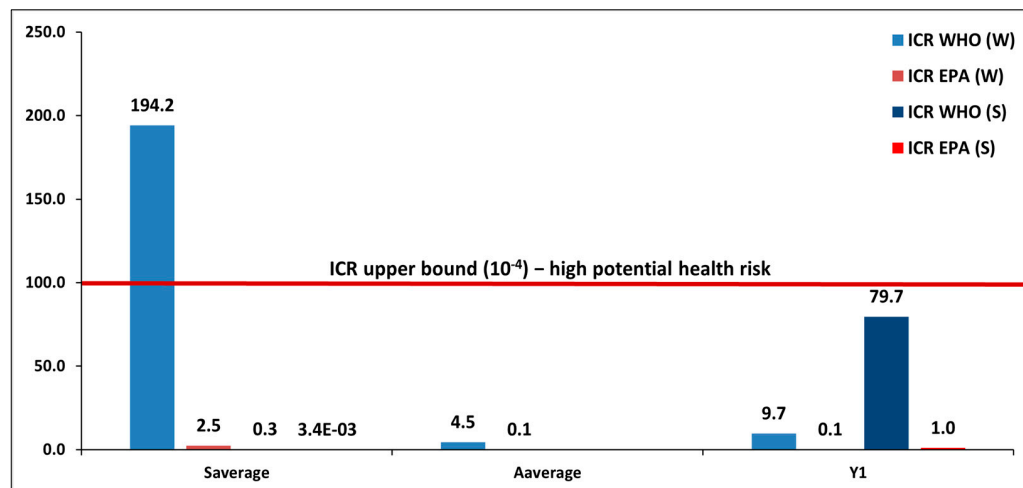


Figure 13. ICR values for both seasons in composite of sites.

ICR calculations were detected in negligible values for the summer period, with ICR according to CalEPA at 3.41×10^{-9} and based on WHO 2.70×10^{-7} . During the winter campaign, the ICR values were calculated to be 2.46×10^{-6} and 1.94×10^{-4} according to CalEPA and WHO, respectively. Hence, if a million people were exposed to 2.23 ng/m^3 TEQ (S_{average} , winter period) for 70 years, 194 and 2.5 persons may have a chance of developing cancer according to WHO and CalEPA, respectively. The calculated ICR values were found to be between ICR values (10^{-6} – 10^{-4}) and in the high potential health risk (WHO: 194) for the people. Conversely, according to the estimated ICR values (2.70×10^{-7} and 3.41×10^{-9}) from the summer campaign (TEQ: 4.15×10^{-3}), the average excess inhalation cancer risks associated with 0.3 and 3.4×10^{-3} per million people, according to WHO and CalEPA, respectively. These values represent lower bounds of the acceptable risk threshold of 10^{-6} .

In the area of Oinofyta, as previously mentioned, the individual sites (A1–A4) were merged into a combined dataset (Table 4, A_{average}) due to the short distances between them and the similarity in concentrations observed. The average values of TEQ and MEQ were calculated to be 0.05 and 0.09 ng/m^3 , respectively. The ICR was calculated to be 4.50×10^{-6} and 1.01×10^{-6} according to WHO and CalEPA, respectively. Subsequently, average estimated excess inhalation cancer risk was 4.5 and 1 cancer cases per million people over an average lifetime of 70 years, for WHO and CalEPA, respectively; both estimations were within the ICR range of potential risk (10^{-6} – 10^{-4}).

According to the results, higher potential health risks were estimated for the winter period across all three studies of interest, with the maximum potential cancer risk being observed at the Municipality of Peloponnese during the winter campaign. When observing Figure 14, attention should be given to the sites within the Municipality of Peloponnese (S1, S2, and S3). To that end, each site was examined separately. This focused approach arises from the consistently high concentrations of PAHs measured at these sites. Consequently, the estimated cancer cases, as indicated by WHO standards, surpassed the upper threshold (10^{-4}), while the EPA's evaluation placed them within the range of potential health risk. Additionally, the variations in PAH concentrations across these sites highlight distinct seasonal patterns and these fluctuations can be attributed to the activities of the olive pomace industries, which are notably active during the winter period.

The TEQ values were higher than the European guideline (TEQ, EU Directive: 1 ng/m^3), while the total ICR value (sum of all stations) indicates that if a million people were exposed approximately to 8 ng/m^3 TEQ for 70 years, eight to nine persons may have a chance of developing cancer.

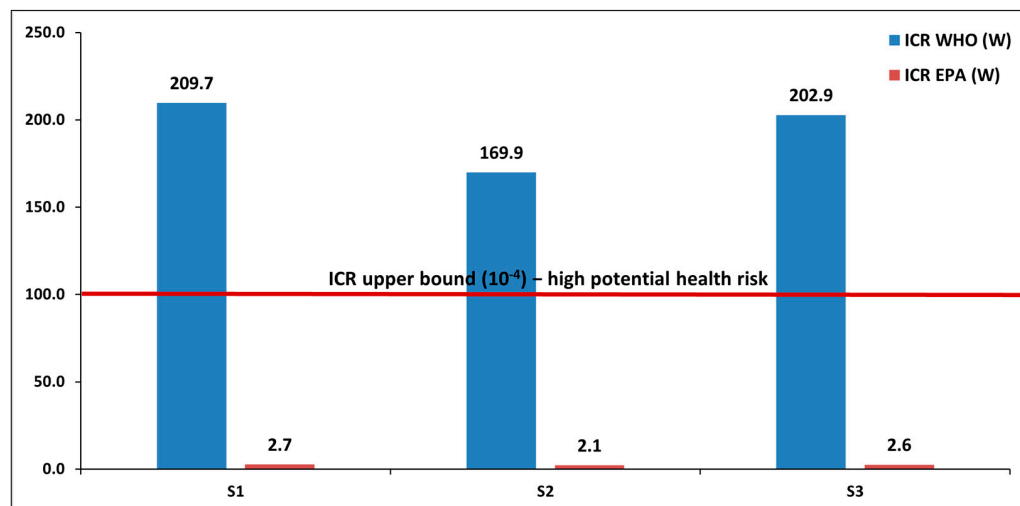


Figure 14. ICR values for both seasons in Municipality of Peloponnese.

In studies conducted at other Greek locations, the average TEQ value was detected at 1.5 ng/m^3 at an urban and traffic site in Thessaloniki, while in the industrialized area of Elefsina it was found to be 2.76 ng/m^3 [54]. ICR average values were calculated as $1.6\text{--}1.7 \times 10^{-6}$ (urban-traffic site) and 3.0×10^{-6} in winter months, respectively. Globally, average TEQ values were found to be equal to 3.6 ng/m^3 in Venice-Mestre, Italy, 31.4 ng/m^3 in Beijing, China, and 0.25 ng/m^3 in Chiang Mai, Thailand, during the winter months, while for one-year sampling conducted in two urban and a rural station in Istanbul, average TEQ values were found to be equal to 2.16 ng/m^3 , 2.65 ng/m^3 , and 1.26 ng/m^3 , respectively [61,62].

3.3.2. Chronic Daily Intake Dose and Cancer Risk Assessment

Risk assessments for short- and long-term daily exposure, as well as potential cancer assessments, are presented below using the approach described previously [20,41]. A key difference from the previous assessments was the consideration of various exposure scenarios for those who have been exposed to pollutants. The sites in Peloponnese (S1, S2, and S3) and Oinofyta (A1, A2, A3, and A4) were merged to S_{average} and A_{average} , respectively, due to the observed minor variations (Table 5).

According to the preceding table, cumulative estimated risk assessments over an 80-year period are presented for individuals, including the different stages of age (Children₀₋₂, Children₂₋₁₆, and Men₁₆₋₈₀), along with the relevant parameters for each scenario (IR, BW, EF, ED, and L). For comparison, the risk assessments for adults over the 80-year period (Children₀₋₂, Children₂₋₁₆, and Men₁₆₋₈₀) were chosen to be presented, as there would be no differences to compare between the different scenarios. As a result, this specific scenario with daily exposure occurring 24 h/day was selected for comparison among the different sites, as it would have higher risk estimations. The results of the estimated risk assessments for all different scenarios are presented subsequently (Supplementary Tables S5–S9). For all three studies of interest, the total inhalation cancer risks were in a lower-bound zero risk (10^{-6}), with higher-risk assessments observed during the winter period. At the Municipality of Peloponnese, the total potential cancer risks were the greatest, then for the Aristotelous and the lowest for the Oinofyta, with lifetime cancer risks of 4.97×10^{-7} , 2.03×10^{-07} , and 1.49×10^{-08} , and 0.05, 0.2, and 0.01 cancer cases per million people, respectively. The estimated risk assessments were predominantly determined by BaP (Figure 15), which accounted for 56.9%, 58.4%, and 65.1% of the total risk assessment across different sites. This was due to the combination of BaP's high cancer potency factor (P) and its higher concentrations observed at all sites.

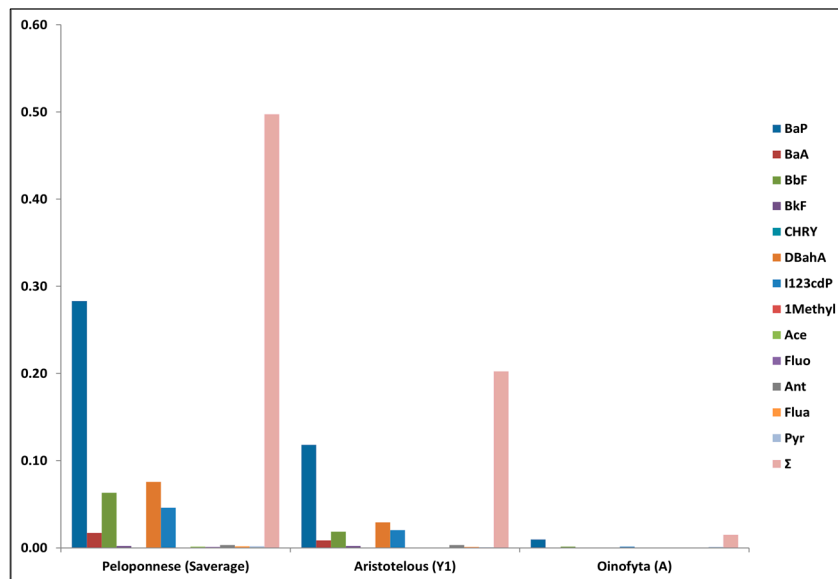


Figure 15. Lifetime cancer risk cases/10⁶ (0–80 y), winter campaign.

Considering the summer campaign, the lifetime cancer risks were significantly lower, due to lower concentrations of the PAHs for both areas (Peloponnese and Aristotelous). The area of Oinofyta lacked measurements for the summer period. For the Municipality of Peloponnese, the total risk assessment for adults over the 80-year period (Children_{0–2}, Children_{2–16}, and Men_{16–80}) was estimated at 2.48×10^{-3} cancer cases per million people, which was significantly lower compared to the winter period (Figure 16). This can be attributed to the activities of the olive pomace industries, which are inactive during this period and are the main source of pollution to the nearby area. Subsequently, a great portion of the PAHs concentrations were under the detection limit and for those that were not, the concentrations were negligible.

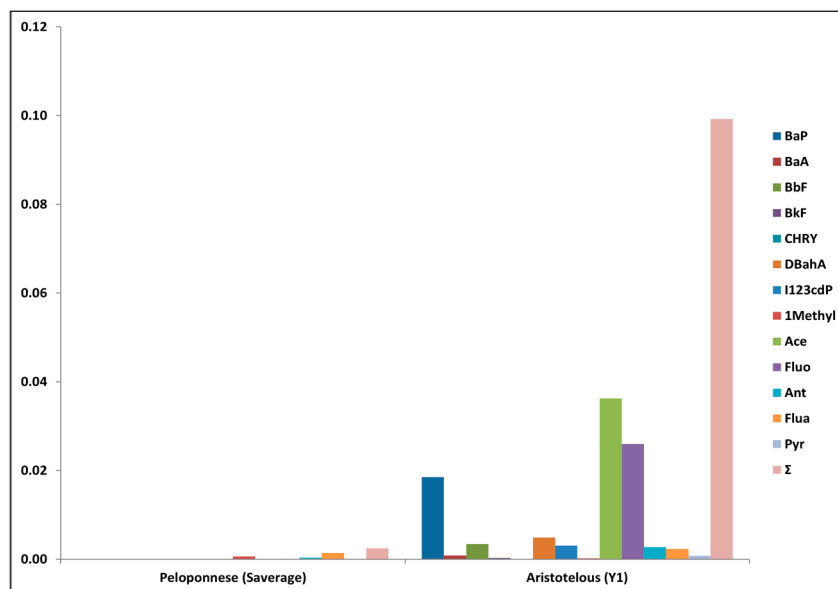


Figure 16. Lifetime cancer risk cases/10⁶ (0–80 y), summer campaign.

As a result, for the Municipality of Peloponnese, the estimated potential risk (2.48×10^{-9}) was found to be significantly lower than the lower-bound zero risk 10^{-6} – 10^{-4} . In the area of Aristotelous, the total risk assessment for adults over the 80-year period (Children_{0–2}, Children_{2–16}, and Men_{16–80}) also was estimated as slightly lower, with

0.1 cancer cases per million people, compared to the winter period. As expected, given Aristotelous’ location in the urban center of Athens, minor differences were anticipated due to seasonal variation. In contrast, the Peloponnese area experienced the absence of olive pomace oil industries during the summer period, while consistent activities were taking place in Aristotelous during both seasons. Likewise, for summer, the estimated potential risk was 1×10^{-7} , which, like the winter period, was significantly lower than the lower-bound zero risk 10^{-6} – 10^{-4} .

In the preceding figure, lifetime cancer risk assessments for the winter period are presented for individuals, including separately the different stages of age for people, as well as the total lifetime cancer risk assessments as described before (adults over the 80-year period, Children_{0–2}, Children_{2–16}, and Men_{16–80}, 24 h/day), for all sites of interest, including the three sites in the Municipality of Peloponnese (S1, S2, and S3) and the S_{average} for comparison purposes. Comparison of sites S1, S2, and S3 in Peloponnese reveals that during the winter period, cancer risk assessments were consistently higher across all sites due to the presence of kernel olive industries, affecting each site equally. Consequently, the composite site S_{average} would offer no discernible difference for comparison purposes in the estimated assessments. Furthermore, Figure 17 illustrates the differences in estimated risks compared to the areas of Aristotelous and Oinofyta, with the latter showing significantly lower risks (Supplementary Tables S6 and S7). At all sites, the cancer risk assessments exhibited equal differences among the different scenarios, with the highest estimated risks observed for men and women exposed 24 h per day, followed by those for men and women exposed for 14 h per day. The lowest risk assessments were for children aged 2–16 and children aged 0–2, respectively. This situation was expected, as despite the differing concentrations across the sites, the same estimated scenarios were used for cancer risk assessments at all sites, resulting in consistent differences. The differences in assessments between scenarios are attributed to variations in exposure doses in every scenario where the person was exposed, different inhalation rates, body weights, and portion of the day that they were exposed (24 or 14 h/day), as well as the duration of exposure in years across different life stages (e.g., Children_{0–2} and Men_{16–80}). During the winter campaign in the Municipality of Peloponnese, the risk assessments for individual PAHs and the total inhalation cancer risk were estimated to be higher compared to the summer. This was anticipated due to the higher concentrations of PAHs, which serve as indicators of the olive kernel industries prevalent during the winter period.

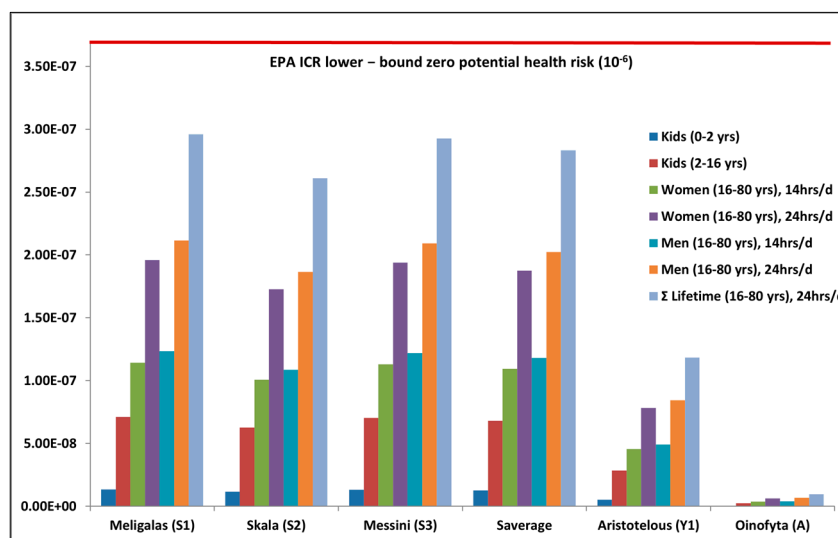


Figure 17. Lifetime cancer risk for all scenarios, winter campaign.

3.4. Source Apportionment

In an attempt to identify the potential PM₁₀ sources and study their differentiation between the three types of environments, two techniques were applied on the available datasets. In particular, diagnostic ratios (DRs) and a PMF model (positive matrix factorization) were used to identify the potential sources and estimate their contribution.

3.4.1. Diagnostic Ratios

Diagnostic ratios (DRs) are among the most significant methods for the identification of sources of atmospheric PAHs; they are widely employed and reliant on the estimation of experimental data. The ratio of specific PAHs to each other or to total PAHs can be utilized to assess the potential of various sources to their atmospheric concentrations by comparing these ratios with those of frequently encountered PAH emissions. However, it must be pointed out that this method should be used with caution as it can be challenging to distinguish between certain sources, such as differentiating between vehicle emissions and those from coal or other biomass fuels [25]. As indicated in Table 6, DRs derived from studies referenced in the literature were applied to the PAH concentrations for the determination of specific areas of interest in this study. For the area of Oinofyta, we presented the aggregated diagnostic ratios ($A_{average}$) due to minor differences observed in the ratios. In general, during the winter period, due to incomplete combustion of organic materials, such as grass, wood, or coal, the combustion process does not proceed efficiently. As a result, the fuel does not burn completely, and various intermediate products, including polycyclic aromatic hydrocarbons (PAHs), are formed. For example, when wood is burned incompletely in a fire, the high temperatures break down the wood’s organic molecules, releasing volatile compounds such as benzene, toluene, ethylbenzene, and xylene (BTEX). These compounds can undergo further reactions and condensation processes in the hot combustion environment to form PAHs, such as naphthalene, phenanthrene, and pyrene. These PAHs are then emitted into the atmosphere as part of the smoke and particulate matter produced by the incomplete combustion process. Once released, they can undergo long-range transport and deposition, leading to their presence in various environmental media, including air, soil, water, and sediments.

Table 6. Diagnostic ratios of the PAHs for all study areas between winter and summer campaigns.

PAH Diagnostic Ratio	Indicator Source	Value Range	S1	S2	S3	A _{average}	Y1
Ant/(Ant + Phe)	Petrogenic sources	<0.1	0.13 (W)	0.18 (W)	0.15 (W)	0.21 (W)	0.23 (W) 0.09 (S)
	Pyrogenic sources	>0.1	N.D. (S)	N.D. (S)	N.D. (S)		
IND/(IND + B[ghi]P)	Petrogenic sources	<0.2	0.49 (W)	0.46 (W)	0.51 (W)	0.32 (W)	0.45 (W)
	Combustion of liquid fuels	0.2–0.50					
Fluo/(Fluo + Pyr)	Grass, wood, and coal combustion	>0.5	N.D. (S)	N.D. (S)	N.D. (S)	0.52 (W)	0.18 (W) 0.69 (S)
	Gasoline	<0.5	0.22 (W)	0.33 (W)	0.45 (W)		
B[a]P/(B[a]P + Chry)	Diesel	>0.5	N.D. (S)	N.D. (S)	N.D. (S)	0.77 (W)	0.60(W) 0.55 (S)
	Petrogenic sources	<0.2	0.40 (W)	0.48 (W)	0.38 (W)		
B[b]Fl / B[k]Fl	Mixed (petrogenic/pyrogenic)	0.2–0.50	N.D. (S)	N.D. (S)	N.D. (S)	0.98 (W)	1.02 (W) 1.34 (S)
	Pyrogenic sources	>0.5	3.21 (W)	3.16 (W)	3.51 (W)		
B[a]P/B[a]P+ B[e]P	Diesel	>0.5	N.D. (S)	N.D. (S)	N.D. (S)	0.41 (W)	0.41 (W) 0.33 (S)
	Fresh particles	~0.5	0.30 (W)	0.36 (W)	0.53 (W)		
Flua/(Flua + Pyr)	Photolysis	<0.5	N.D. (S)	N.D. (S)	N.D. (S)	0.52 (W)	0.54 (W) 0.53 (S)
	Petrogenic sources	<0.4	0.44 (W)	0.43 (W)	0.45 (W)		
B[a]P/B[ghi]P	Liquid fossil fuel burning	0.4–0.5	0.41 (S)	0.42 (S)	0.69 (S)	0.37 (W)	0.42 (W) 0.26 (S)
	Coal, wood, and grass burning	>0.5	0.41 (W)	0.51 (W)	0.37 (W)		
IND/B[ghi]P	Non-traffic emissions	<0.6	0.99 (W)	0.89 (W)	1.08 (W)	0.48 (W)	0.90 (W) 0.55 (S)
	Traffic emissions	>0.6	N.D. (S)	N.D. (S)	N.D. (S)		
	Gasoline	<0.4	N.D. (S)	N.D. (S)	N.D. (S)		
	Diesel	~1	N.D. (S)	N.D. (S)	N.D. (S)		

Table 6. Cont.

PAH Diagnostic Ratio	Indicator Source	Value Range	S1	S2	S3	A _{average}	Y1
B[a]A/ (B[a]A + Chry)	Petrogenic sources	<0.2	0.21 (W)	0.32 (W)	0.25 (W)	0.28 (W)	0.43 (W)
	Petroleum and fuel oil combustion	0.2–0.35	N.D. (S)	N.D. (S)	N.D. (S)		0.29 (S)
	Coal, wood, and grass combustion	>0.35					
Flua/Pyr	Petrogenic sources	<1	0.79 (W)	0.76 (W)	0.82 (W)	1.18 (W)	2.19 (W)
	Combustion of solid fuel	>1	0.69 (S)	N.D. (S)	0.69 (S)		1.44 (S)
Pyr/B[a]P	Gasoline	~1	0.45 (W)	0.53 (W)	0.47 (W)	0.39 (W)	0.32 (W)
	Diesel	~10	N.D. (S)	0.71 (S)	N.D. (S)		2.35 (S)
LMW/HMW	Pyrogenic sources (coal, grass, and burning of wood)	<0.1	0.17 (W)	0.23 (W)	0.58 (W)	1.29 (W)	0.11 (W)
	Petrogenic sources (fuel or one refined petroleum product)	>0.1	0.15 (S)	N.D. (S)	N.D. (S)		6.13 (S)
Phe/Ant	Combustion of solid fuel	<10	N.D. (W)	N.D. (W)	5.84 (W)	24.48 (W)	5.01 (W)
	Petrogenic	>10	N.D. (S)	N.D. (S)	N.D. (S)		63.50 (S)
Total Index (Flua, Pyr, Ant, Phe, B[a]A, Chry, IND, B[ghi]P)	Low-temperature source (petroleum)	<4	1.99 (W)	2.58 (W)	2.13 (W)	3.59 (W)	5.04 (W)
	High-temperature source (combustion)	>4	N.D. (S)	N.D. (S)	N.D. (S)		2.78 (S)
СПАΥ/ΣΠΑΥ	Combustion	~1	0.76 (W)	0.74 (W)	0.61 (W)	0.46 (W)	0.81 (W)
			0.48 (S)	0.52 (S)	0.44 (S)		0.65 (S)

Winter Period

Specifically at the Municipality of Peloponnese, the estimated ratios of Flua/Pyr and LMW/HMW indicated that PAHs during the winter period originated from petrogenic sources, although several estimated ratios (IND/(IND + B[ghi]P), B[a]P/(B[a]P + Chry), B[a]A/(B[a]A + Chry) were observed, indicating a combination of petrogenic/pyrogenic sources for the winter period. It is important to note that both IND/(IND + B[ghi]P) and B[a]P/(B[a]P + Chry) were near the upper limit of the ratio range, which indicates strong relation with pyrogenic sources as well, with the only exception in S3 for winter period being the DR for IND/(IND + B[ghi]P), indicating grass, wood, and coal combustion. Additionally, the Flua/(Flua + Pyr) ratio suggested potential liquid fossil fuel burning as a source. Considering pyrogenic sources, grass, wood, and coal combustion for winter period were indicated from Ant/(Ant + Phe) and Phe/Ant. Specifically, the DRs for Phe/Ant were calculated only for S3 (combustion of solid fuel), while for the sites S1 and S2 there were not concentrations for the Ant or they were under the detection limit (Table 3). Furthermore, the DRs from B[b]Fl / B[k]Fl and IND/B[ghi]P indicated diesel as potential source for all sites (S1, S2, and S3). In contrast, the ratio of Fluo/(Fluo + Pyr) revealed gasoline as an indicator source. For the Fluo/(Fluo + Pyr) ratio to indicate diesel as a potential source, this requires Fluo concentrations to be higher than Pyr concentrations. In our study, the concentrations of Pyr for the summer and the winter campaign were the same for the Municipality of Peloponnese, despite the different activities and potential sources among seasons. As a result, the gasoline as indicator source was attributed to the low concentrations of Fluo for the winter period. The Pyr/B[a]P diagnostic ratios also suggested gasoline as a potential source, likely due to the presence of B[a]P concentrations. For all sites of Peloponnese, B[a]P/B[ghi]P ratio revealed non-traffic emissions as an indicator source. The B[a]P/B[a]P + B[e]P ratio indicated photolysis for the sites S1 and S2, while for site S3, fresh particles were demonstrated. The total index ratio also suggested a low-temperature source (petroleum) as a potential source for all sites (S1, S2, and S3).

In the area of Oinofyta, the fluctuation profile of PAHs primarily indicated traffic-related sources as DRs, aligning with the proximity of all sampling stations nearby the national highway. In particular, ratios of Fluo/(Fluo + Pyr), IND/B[ghi]P and Pyr/B[a]P indicated gasoline vehicles' emissions. Concurrently, the B[a]P/B[ghi]P ratio revealed non-traffic emission in a nearby area. Pyrogenic sources, grass, wood, and coal combustion, were

demonstrated by $\text{Ant}/(\text{Ant} + \text{Phe})$, $\text{B[a]P}/(\text{B[a]P} + \text{Chry})$, $\text{Flua}/(\text{Flua} + \text{Pyr})$, and Flua/Pyr ratios, while $\text{IND}/(\text{IND} + \text{B[ghi]P})$ and $\text{B[a]A}/(\text{B[a]A} + \text{Chry})$ indicated petroleum and fuel oil combustion. The $\text{B[b]Fl}/\text{B[k]Fl}$ ratio pointed to diesel as an indicator source. In addition, LMW/HMW and Phe/Ant were indicated as petrogenic sources, such as fuel or one refined petroleum product, a situation that can be attributed to the industrial activities in the nearby area. Photolysis was demonstrated for the area of Oinofyta. The total index ratio also suggested a low-temperature source (petroleum) as a potential indicator source. Considering the center of Athens (Aristotelous), during the winter period, non-traffic-related sources (a mixture of gasoline and diesel vehicles), diesel sources (central heating/vehicles), and possibly biomass combustion sources were identified. Notwithstanding that, the DRs $\text{IND}/\text{B[ghi]P}$ and $\text{B[b]Fl}/\text{B[k]Fl}$ were indicated as diesel sources, and the $\text{Fluo}/(\text{Fluo} + \text{Pyr})$ and $\text{Pyr}/\text{B[a]P}$ showed gasoline sources. Pyrogenic and combustion of solid fuel as indicator sources were demonstrated by the $\text{Ant}/(\text{Ant} + \text{Phe})$, $\text{B[a]P}/(\text{B[a]P} + \text{Chry})$, $\text{Flua}/(\text{Flua} + \text{Pyr})$, $\text{B[a]A}/(\text{B[a]A} + \text{Chry})$, LMW/HMW, Flua/Pyr , and Phe/Ant ratios, and the $\text{IND}/(\text{IND} + \text{B[ghi]P})$ ratio indicated combustion of liquid fuels. For both seasons, the DR $\text{B[a]P}/\text{B[a]P} + \text{B[e]P}$ indicated photolysis as an indicator source.

Summer Period

During the summer campaign in the Municipality of Peloponnese, significant indications of petrogenic sources such as fuel or refined petroleum products were also identified through diagnostic ratios (Phe/Ant and LMW/HMW). However, a considerable portion of PAHs was either absent or present at concentrations below the detection limit during the summer period, for the three areas S1, S2, and S3, respectively. As a result, several DRs could not be applied for the identification of potential sources. This could be attributed to the absence of industrial activities related to kernel olive processing. Furthermore, liquid fossil fuel burning as an indicator source was demonstrated by the $\text{Flua}/(\text{Flua} + \text{Pyr})$ ratio. Although, in the winter period either gasoline or diesel were indicated as potential sources, during the summer period, diesel was demonstrated as an potential source. In the area of Aristotelous, significant indications of pyrogenic sources were also identified for the summer period through several diagnostic ratios ($\text{B[a]P}/(\text{B[a]P} + \text{Chry})$, $\text{Flua}/(\text{Flua} + \text{Pyr})$, and Flua/Pyr). The ratios of $\text{Ant}/(\text{Ant} + \text{Phe})$, LMW/HMW, and Phe/Ant suggested petrogenic sources during the summer campaign, contrasting with the winter period, where they indicated pyrogenic sources. This situation can be attributed to seasonal variations in residents' activities.

Although the diagnostic ratio of $\text{B[a]P}/\text{B[ghi]P}$ for the summer campaign demonstrated non-traffic emissions, as well as for the winter campaign, respectively, it is worth mentioning that for the winter period there were fluctuations for the diagnostic ratio between traffic, or not, emissions (Figure 18). As a result, in spite of the majority of the individual ratios indicating non-traffic emissions (<0.6), a significant portion of the sampling days showed diagnostic ratios above the value of 0.6 ($\text{B[a]P}/\text{B[ghi]P}$), corresponding to traffic sources. This underscores the complexity of the phenomenon and highlights that the sources of emissions can vary from day to day, adding further intricacy and making the identification of the potential sources more challenging. This is something worth mentioning, as most studies on source apportionment that utilize diagnostic ratios focus on the averages of the indicated DRs in their results and discussions. This approach may oversimplify and omit information by comparing averaged DRs rather than examining individual ratios for each day separately.

An illustrative example of this phenomenon is observed in the DRs for $\text{B[a]A}/(\text{B[a]A} + \text{Chry})$ and Flua/Pyr for Aristotelous. During the summer period, the averaged DR for $\text{B[a]A}/(\text{B[a]A} + \text{Chry})$ indicated petroleum and fuel oil combustion, while the averaged Flua/Pyr ratio suggested combustion of solid fuel. Upon closer examination of the data in Figure 19, it becomes evident that individual DRs for Flua/Pyr were divided between the potential sources (combustion of solid fuel and petrogenic), with the majority of the measured days (25 out of 36) indicating petrogenic sources, as their ratios were below the

value of 1. However, the averaged DRs for Flua/Pyr were calculated above the value of 1 (1.44, Table 6), as depicted in Figure 19. This discrepancy arises because although individual days with DR values higher than 1 were in the minority (11 out of 36), their values were sufficiently high to influence the averaged DR. Concluding this, the combustion of solid fuel emerges as a potential source based on Flua/Pyr's DR, while the potential indicator sources identified by B[a]An/(B[a]An + Chry were a mix of coal, wood, and grass combustion, as well as petroleum and fuel oil combustion. Comparing this with Figure 20 from the winter period, for both seasons there were activities from a combination of petrogenic and combustion of solid fuel sources (Flua/Pyr). However, the indicator source demonstrated by B[a]An/(B[a]An + Chry during the winter period was mainly coal, wood, and grass combustion, in contrast with the summer period.

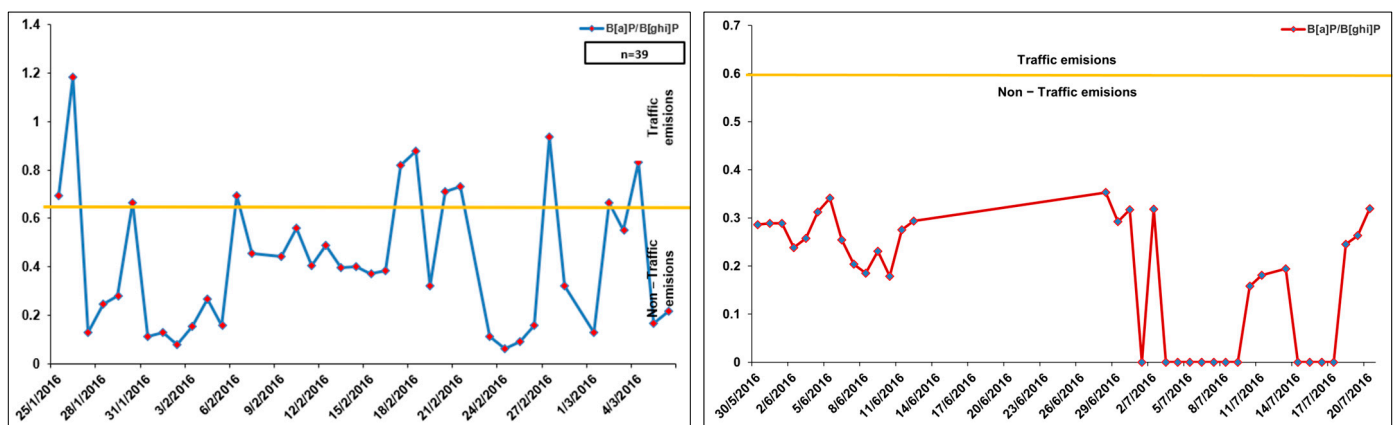


Figure 18. Seasonal variation of traffic emissions (Aristotelous) of B[a]P/B[ghi]P.

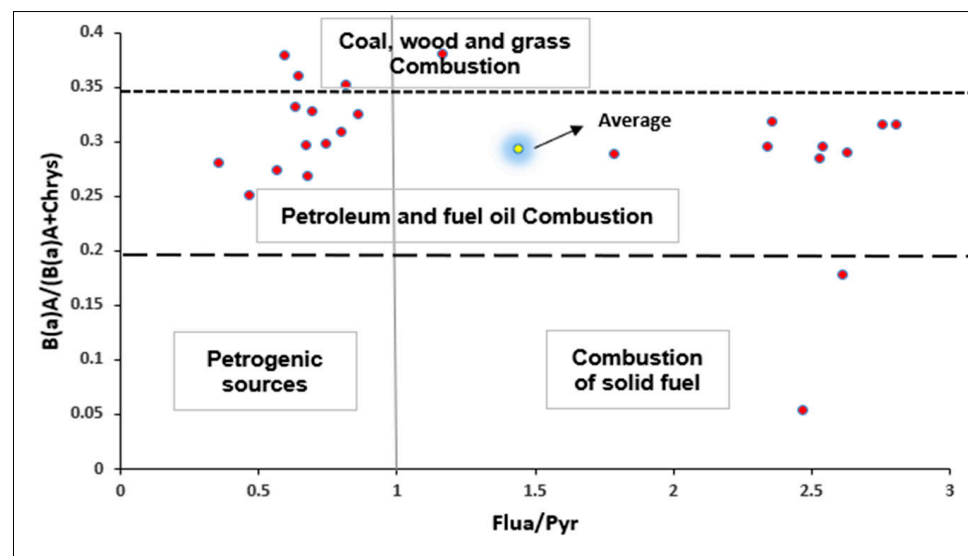


Figure 19. Cross-plot for DR of B[a]A/(B[a]A + Chry) and Flua/Pyr, summer campaign (Aristotelous).

Comparing this with Figure 20 from the winter period, for both seasons, there were activities from a combination of petrogenic and combustion of solid fuel sources (Flua/Pyr). However, the indicator source demonstrated by B[a]An/(B[a]An + Chry during the winter period was mainly coal, wood, and grass combustion, in contrast with the summer period. For the summer campaign, the presence of Aristotelous diesel as a potential source was indicated by DRs of Fluo/(Fluo + Pyr), B[b]Fl / B[k]Fl and IND/B[ghi]P.

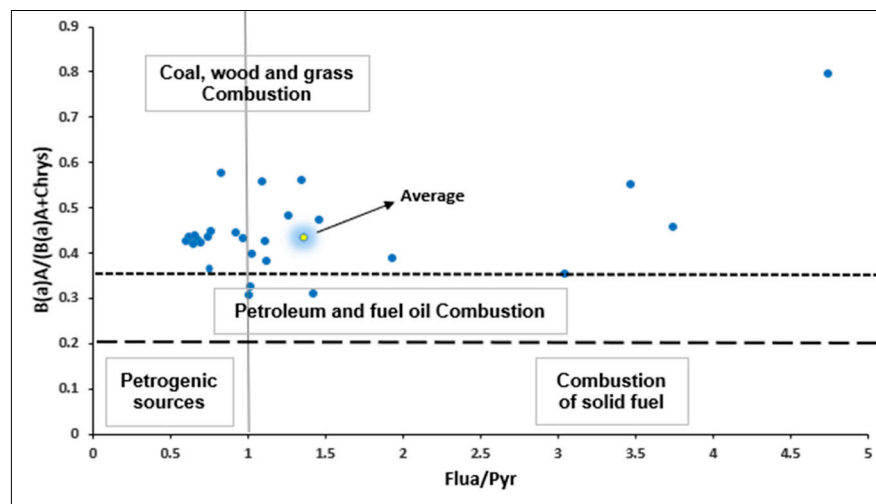


Figure 20. Cross-plot for DR of B[a]A/(B[a]A + Chry) and Flua/Pyr, winter campaign (Aristotelous).

Furthermore, the total index in Aristotelous for both seasons indicated different potential sources, highlighting the varying activities taking place. During the summer campaign, the total index demonstrated a low-temperature source (petroleum) as primary source, while for the winter period, the diagnostic ratio suggested a high-temperature source (combustion). It is worth mentioning that for the winter period, the indicator source from total index remained the same until date 23 February 2016, when the indicator source changed. For the following 13 consecutive days, petroleum was demonstrated as the indicator source (Figure 21).

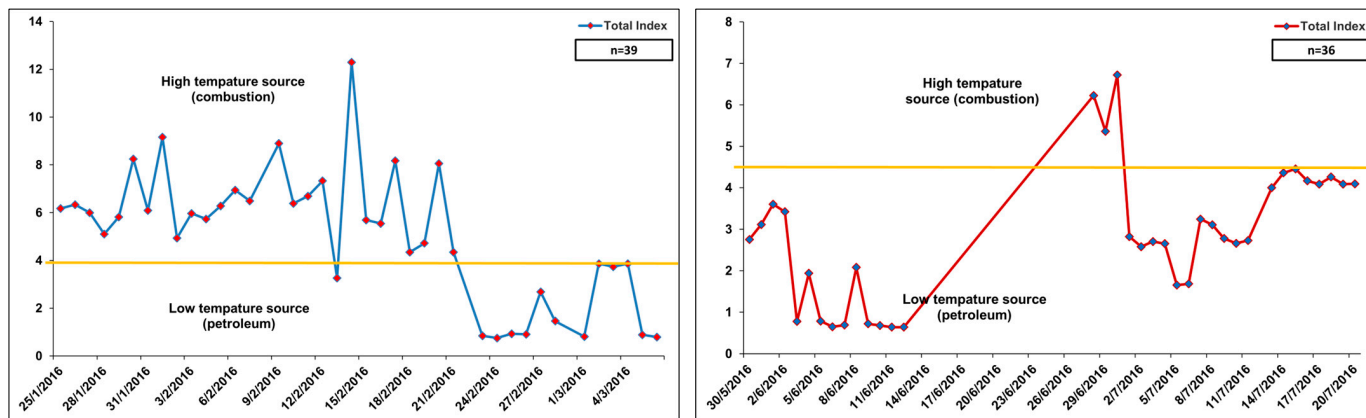


Figure 21. Seasonal variation of total index ratio (Aristotelous).

3.4.2. PMF Results for Municipality of Peloponnese

For the Municipality of Peloponnese the chemical elements used as input in the model were six ions (Na^+ , K^+ , Mg^{2+} , Ca^{2+} , NO_3^- , SO_4^{2-}), mental and organic carbon (EC, OC), and six heavy PAH species (BghiP, IND, BbF, BkF, BaP, BeP). The resolved sources were qualitatively identified by the trace markers shown in the mass profiles (Figure 22). Figure 23 presents the factors' percentage contributions to PM.

Factor 1 is characterized by high percentages of nitrate (62%) and sulfate (43%) ions as well as an amount of organic carbon (25%), which reveal a secondary aerosol source that can be associated with traffic exhaust emissions [63–65]. This factor accounts for 15% of the measured PM_{10} at the Municipality of Peloponnese.

Factor 2 reveals a mixed source of natural origin: mineral dust, as it is traced by significant percentages (>70%) of Mg^{2+} and Ca^{2+} , probably mixed with sea salt due to a high percentage of Na (77%). This factor contributes 23% of the measured PM_{10} .

Factor 3, which is characterized by similar percentages of OC and EC (OC/EC~1), as well as a significant percentage of sulfate ion (37%), corresponds to traffic emissions, as also found in similar studies [63,65–67]. Furthermore, the presence of BaP in combination with sulfate ion indicates industrial emissions, which in the absence of elemental species in the analysis, cannot be further specified. This factor contribution to PM₁₀ is 37%.

Factor 4 reveals the biomass/wood combustion source due to the high percentage of K⁺ (>50%) and the presence of OC (17%) and BaP (13%), which are characteristic combustion tracers [68].

Factor 5 is strongly associated with the heavy PAH species, BbF, BkF, BeP, BghiP, IND (100%), and moderate contributions of OC and EC; thus, it can be associated with diesel emissions (heavy vehicles/residential heating) [69]. This diesel emissions factor contributes 9% of the measured PM₁₀.

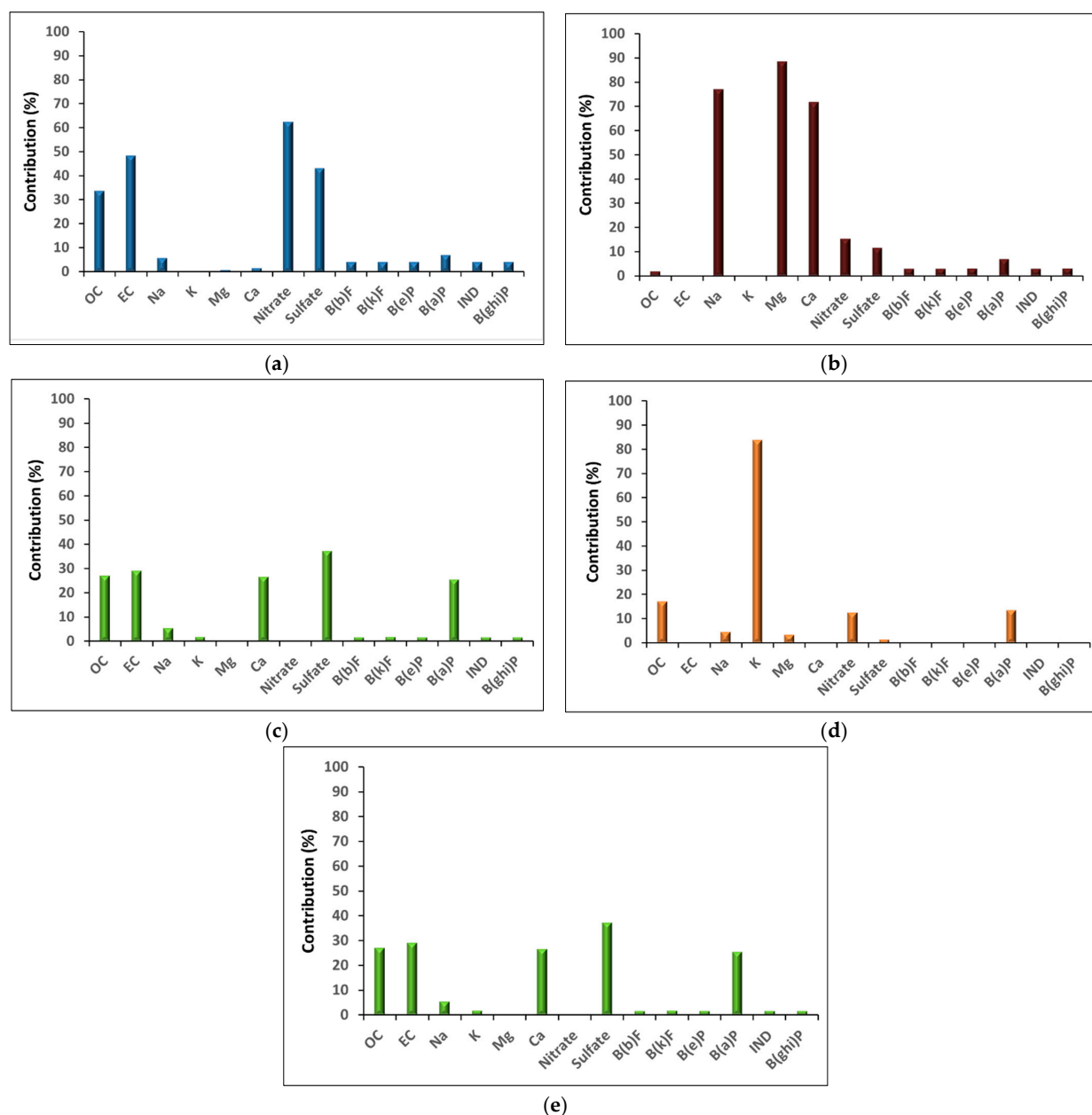


Figure 22. Sources and contribution of each chemical element separately for factors 1–5. (a) Factor 1. Secondary aerosols/traffic; (b) Factor 2. Natural sources; (c) Factor 3. Traffic/industrial emissions; (d) Factor 4. Biomass/wood combustion; (e) Factor 5. Diesel emissions (traffic/central heating).

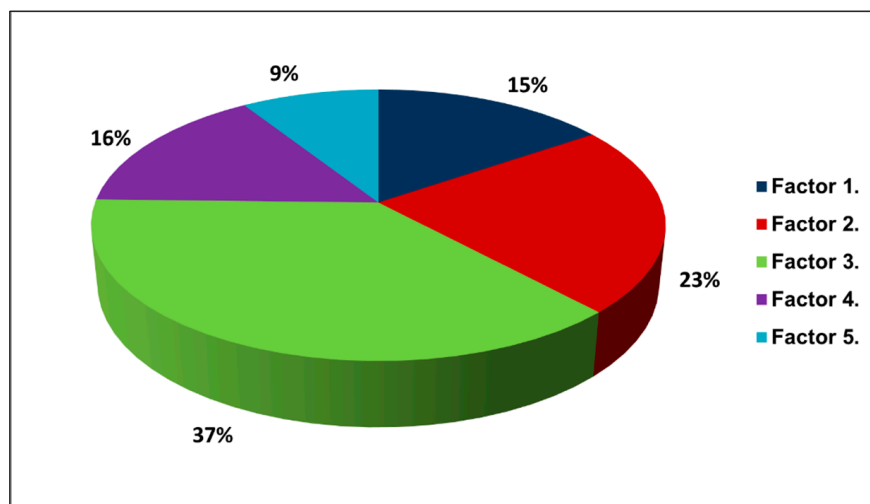


Figure 23. Percentage contribution of each factor source for Municipality of Peloponnese. Factor 1: Secondary aerosols/traffic; Factor 2: Natural sources; Factor 3: Traffic/industrial emissions; Factor 4: Biomass/wood combustion; Factor 5: Diesel emissions (traffic/domestic heating).

3.4.3. PMF Results for Aristotelous

For Aristotelous, the chemical species injected to the model were six ions (Na^+ , K^+ , Mg^{2+} , Ca^{2+} , NO_3^- , SO_4^{2-}), elemental and organic carbon (EC and OC), seven metals (V, Ni, Ti, Fe, Cu, Zn, Pb), and six heavy PAH species (BghiP, IND, BbF, BkF, BaP, BeP). Figure 24 presents the sources and the contribution of chemical elements to each, individually. Figure 25 presents the factors' percentage contributions to PM for the Aristotelous area.

Factor 1 reveals a source of crustal origin (Ca^{2+} , $\text{Ti} > 50\%$) enriched with traffic/industrial emissions tracers (Fe, EC, Zn, Cu, Pb) and therefore corresponds to road dust [65,70]. This factor contributes 19% of the measured PM_{10} at the traffic site of Athens.

Factor 2 is associated with significant ($> 50\%$) percentages of V, Ni, SO_4^{2-} , BghiP, IND, BbF, BkF, and BaA, which, in combination with the presence of Cu, Zn, Pb, OC, EC, Fe, and K, indicates fuel oil combustion and exhaust traffic emissions [69]. This factor accounts for 18% of the measured PM_{10} .

Factor 3 is characterized by nitrate, sulfate, and ammonium ions, which reveals a secondary aerosol source probably mixed with a sea salt source (Na^+ , Mg^{2+}).

Factor 4 corresponds to combustion sources as it is characterized by high percentages of K^+ , DBA ($> 50\%$), BaP, and OC. In particular, K^+ and BaP are characteristic tracers of wood combustion, which was intense during the winter period (domestic heating). This factor accounts for the quite high percentage of 21% of the measured PM_{10} [68].

Factor 5 is associated with the two carbonaceous fractions (OC and EC; OC/EC = 0.9) and sulfate ion, which indicates traffic-related sources. Additionally, high percentages of Pyr, BaA, and Bap correspond to a traffic gasoline source [64]. This factor accounts for the quite high percentage of 30% of the measured PM_{10} at the traffic site of Athens.

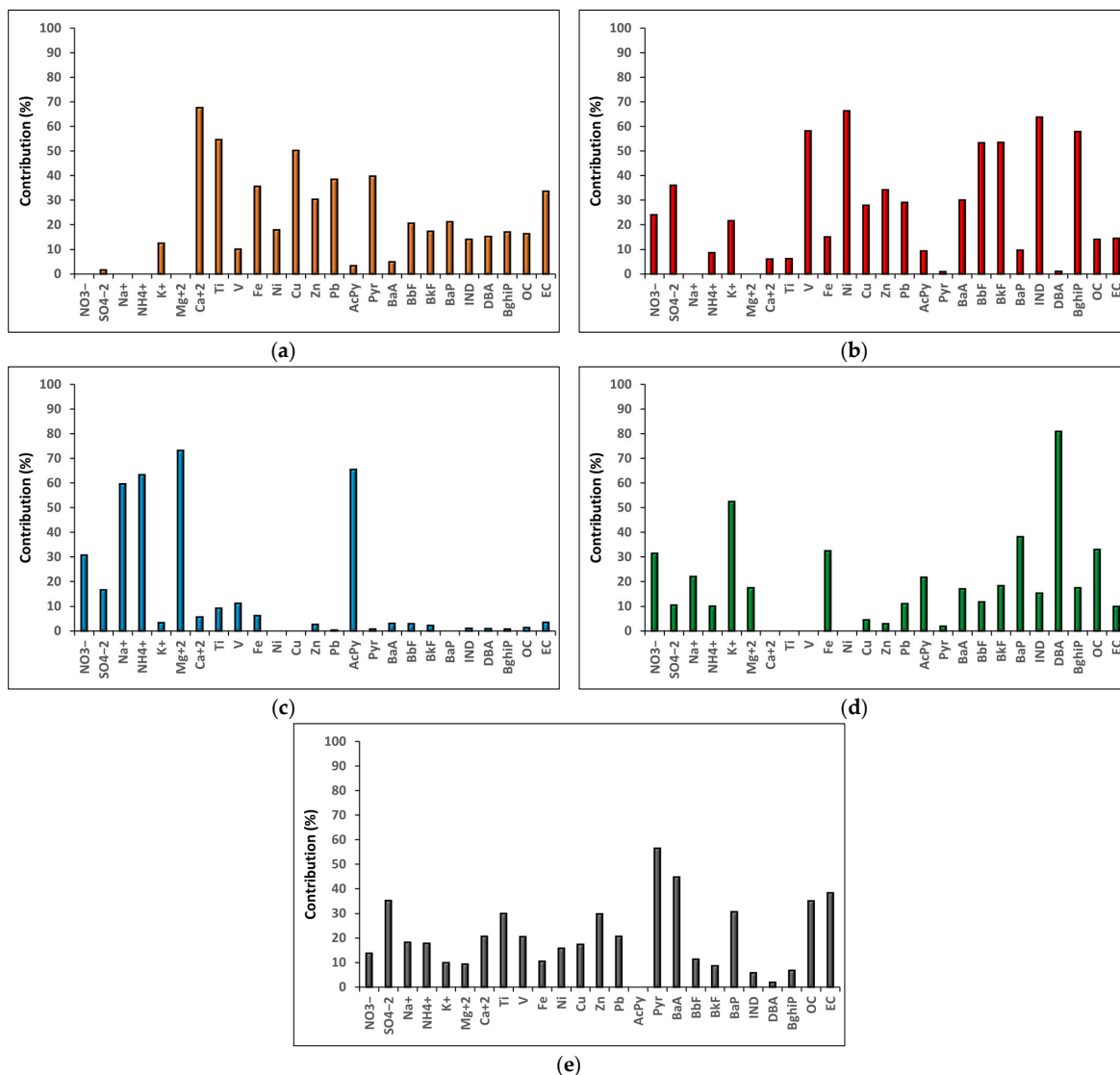


Figure 24. Sources and contribution of each chemical element separately for factors 1–5. (a) Factor 1. Road dust; (b) Factor 2. Fuel oil combustion/traffic diesel; (c) Factor 3. Sea salt/secondary aerosols; (d) Factor 4. Biomass/wood combustion; (e) Factor 5. Traffic gasoline.

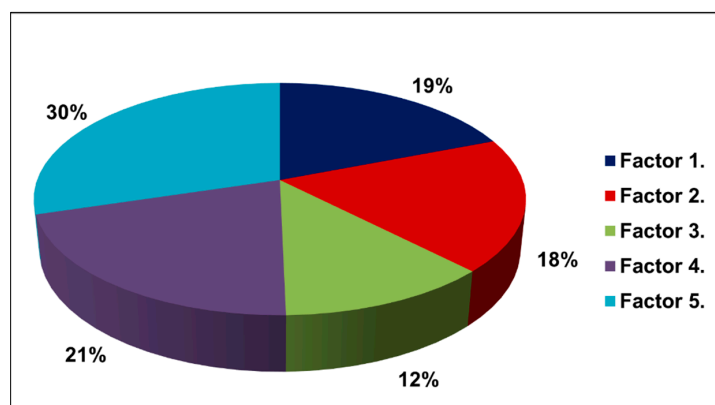


Figure 25. Percentage contribution of each factor source for Aristotelous. Factor 1. Road dust; Factor 2. Fuel oil combustion/traffic diesel; Factor 3. Sea salt/secondary aerosols; Factor 4. Biomass/wood combustion; Factor 5. Traffic gasoline.

4. Conclusions

The aim of this study was the assessment of the variance in PAHs concentrations as well as the identification and estimation of the contribution of the main PAHs sources in three areas of different characteristics: an area in Peloponnese characterized by intense olive-production activity, the industrialized zone of Oinofyta, and an urban site of heavy traffic in the Athens city center (Aristotelous). For the scope of the study, the carcinogenic equivalent concentration (TEQ), inhalation cancer risk (ICR), and lifetime cancer risk (R) were estimated; in addition, two source apportionment methods were applied (DRs and PMF model). According to the results for PM₁₀ concentration and its chemical composition for PAHs, the study areas were characterized by diverse sources and activities, yielding findings that include assessments of the potential health effects from the pollutants for the residents of the areas of interest:

- The maximum PM₁₀ mass concentration and the percentage of exceedances (daily limit value by the European Union 50 µg/m³) was observed at the sites within the Municipality of Peloponnese (Meligalas: 13%, Skala: 27%, Messini: 11%) during the winter season. The latter is attributed to both biomass burning (domestic heating, agriculture activities) and the operation of olive pomace oil industries during winter. The same trend was observed for Σ₂₂PAHs, ΣCOMPAHs, and ΣCANPAHs, possibly associated with the same sources.
- Indicatively, the average concentrations of B(a)P in the areas of the Municipality of Peloponnese during the winter season exceeded the annual limit of 1 ng/m³ (according to EU Directive 2004/107/EC), while the corresponding average value in the area of Aristotelous was 0.51 ng/m³. In the summer, B(a)P was undetectable or negligible in all areas. The elevated levels at Peloponnese area also imply the contribution of the emissions from olive pomace oil industries.
- The highest potential cancer risk (TEQ and ICR) was observed at the Municipality of Peloponnese during the winter season. The TEQ values were higher than the European guideline (TEQ, EU Directive: 1 ng/m³). This indicates that the citizens of the Municipality of Peloponnese had greater exposure dose to a harmful mixture of PAHs during the winter months compared to summer and the other study areas.
- In the center of Athens (Aristotelous), for both seasons, the number of cancer cases per million people were within the ICR range of potential health risk (10⁻⁶–10⁻⁴), according to WHO and EPA, with the estimated ICR for summer being lower. At the Municipality of Peloponnese during the winter campaign, the estimated cancer cases by WHO surpassed the upper threshold (10⁻⁴), while the EPA evaluation placed them within the range of potential health risk.
- The total inhalation lifetime cancer risks were close to a lower-bound zero risk (10⁻⁶) for all three areas of interest (Peloponnese, Aristotelous, and Oinofyta), which further underscores the low concentration of PAHs. Higher risk assessments were observed during the winter period. Likewise, for summer, the estimated potential risks were lower than the lower-bound zero risk. Lifetime cancer risk for all scenarios demonstrate the differences in PAHs concentrations for the estimated risks compared to the areas of Aristotelous and Oinofyta, with the latter showing significantly lower risks, mainly due to the lower concentrations.
- The cancer risk assessments exhibited equal differences among the different scenarios for all study areas, with the highest estimated risks observed for men and women exposed 24 h per day, followed by those for men and women exposed for 14 h per day. The lowest risk assessments were for children aged 2–16 and children aged 0–2, respectively. The differences observed in the assessments between scenarios were anticipated and can be attributed to variations in exposure doses, inhalation rates, body weights, and portion of the day they were exposed (24 or 14 h/day), as well as the duration of years of exposure across various life stages (e.g., Children₀₋₂ and Men₁₆₋₈₀).

- According to PMF, the prevailing sources of PM₁₀ at the Municipality of Peloponnese were biomass/wood combustion and traffic/industrial emissions. In Aristotelous, traffic-related sources (gasoline emissions and road dust) and biomass/wood combustion emerged as the most significant factors contributing to the measured PM₁₀ levels.
- The activities of the olive pomace industries during winter period contributed significantly to various indicator sources from DRs (petrogenic, mixture of gasoline and diesel; high-molecular-weight PAHs were the most abundant). In the summer period, a considerable portion of PAHs was either absent or present at concentrations below the detection limit. The latter could be attributed to the absence of industrial activities related to olive pomace oil industries and the biomass burning for domestic heating in the nearby area.
- In the industrial zone, DRs indicated petrogenic sources, pyrogenic activities, and a mixture of gasoline and diesel emissions from vehicles. In the center of Athens, a wide-ranging profile of PAHs sources was demonstrated by DRs for both seasons. Non-traffic emissions were indicated for both seasons, with lower ratio for the summer period. Significant fluctuations in individual DRs were observed during the winter period, contrasting with the summer period.

5. Future Study

A common method of using DRs needs to be applied to relevant studies, resulting in better comparability among the results of different studies. This refers to which DRs are used in each study and the interpretation of DRs when there are different indicator sources for the same sources (e.g., petrogenic or pyrogenic sources). Instead of examining individual ratios for each day separately, most studies on source apportionment that utilize diagnostic ratios focus on the averages of the indicated DRs, a situation that should receive more attention. Gathering air pollution data with higher temporal resolution (daily and seasonal variations) and spatial resolution (a network of sampling sites) would enhance the accuracy of risk assessments by accounting for the variability in environmental factors and human activities. To achieve this, the scientific community should concentrate on developing more comprehensive mathematical models and approaches that consider all parameters linking air pollution exposure to population health. This includes addressing the limited number of sampling sites, accounting for seasonal variations, changes in population vulnerabilities, and lifestyle characteristics, as well as incorporating source apportionment and accurate identification of pollution sources to enhance the reliability of the assessments.

Supplementary Materials: The following supporting information can be downloaded at: <https://www.mdpi.com/article/10.3390/atmos15080938/s1>; Equation (S1). Total index, Bootdee et al., 2016 [35]; Table S1. Minimum–maximum (mean) and total PAHs concentrations (ng/m³) adsorbed to ambient PM₁₀ (ng/m³) for winter campaign in Municipality of Oichalia–Messini; Table S2. Minimum–maximum (mean) and total PAHs concentrations (ng/m³) adsorbed to ambient PM₁₀ (ng/m³) for summer campaign in Municipality of Oichalia–Messini; Table S3. Minimum–maximum (mean) and total PAHs concentrations (ng/m³) adsorbed to ambient PM₁₀ (ng/m³) in Aristotelous and Oinofyta for both seasons; Table S4. LOD and LOQ of the chromatographic method for the determination of PAHs; Table S5. Estimated cancer risk of humans due to inhalation of PAHs for Municipality of Peloponnese, winter period; Table S6. Estimated cancer risk of humans due to inhalation of PAHs for Municipality of Aristotelous, winter period; Table S7. Estimated cancer risk of humans due to inhalation of PAHs for Municipality of Oinofyta, winter period; Table S8. Estimated cancer risk of humans due to inhalation of PAHs for Municipality of Peloponnese, summer period; Table S9. Estimated Cancer risk due to inhalation of PAHs for Municipality of Aristotelous, summer period.

Author Contributions: Conceptualization, T.M. and D.S.; methodology, T.M., M.P. and M.D.; software, D.S.; validation, T.M., D.S. and M.P.; formal analysis, D.S., M.P. and M.D.; investigation, M.P., M.D. and P.P.; resources, T.M.; data curation, D.S., M.P. and D.S.; analysis, M.D., D.B., P.P. and K.B.; writing—original draft preparation, M.P. and M.D.; writing—review and editing, D.S. and T.M.; visualization, M.P. and D.S.; supervision, T.M. and D.S.; project administration, T.M.; funding acquisition, T.M. All authors have read and agreed to the published version of the manuscript.

Funding: This research received no external funding.

Institutional Review Board Statement: Not applicable.

Informed Consent Statement: Not applicable.

Data Availability Statement: The original contributions presented in the study are included in the article/Supplementary Materials, further inquiries can be directed to the corresponding author/s.

Conflicts of Interest: The authors declare no conflicts of interest.

Appendix A

Table A1. Detailed information on sampling areas.

Sampling Name Code	Characteristics of Sampling Point	Region	Coordinates	
			X	Y
S1	Terrace of ground floor of Meligala fire station	Meligala	37°13'19" N	21°58'35" E
S2	Terrace of the ground floor store in Skala	Skala	37°12'06" N	21°59'50" E
S3	City Hall of Messinia	Messinia	37°02'45" N	22°00'26" E
Y1	Aristotelous, Center of Athens	Athens	37°59'36" N	23°43'44" E
A1	Building of Fire Department in Oinophyta	Oinophyta	38°18'35" B	23°38'24" A
A2	Building of FEST Industry in Oinophyta	Oinophyta	38°19'0" B	23°39'10" A
A3	Building of PURATOS Industry	Oinophyta	38°18'36" B	23°37'9" A
A4	Building of SARANTIS Industry	Oinophyta	38°18'30" B	23°39'29" A

References

- United Nations Environment Programme. Pollution Action Note—Data You Need to Know. Available online: <https://www.unep.org/interactives/air-pollution-note/> (accessed on 25 May 2024).
- WHO. WHO Global Air Quality Guidelines: Particulate Matter (PM_{2.5} and PM₁₀), Ozone, Nitrogen Dioxide, Sulfur Dioxide and Carbon Monoxide. Licence: CC BY-NC-SA 3.0 IGO; World Health Organization: Geneva, Switzerland, 2021; Available online: <https://www.who.int/publications/i/item/9789240034228> (accessed on 25 May 2024).
- European Environment Agency. Outdoor Air Quality in Urban Areas. Available online: <https://www.eea.europa.eu/airs/2018/environment-and-health/outdoor-air-quality-urban-areas> (accessed on 25 May 2024).
- Saldarriaga, H.; Villalobos, R.; Solano, G.; Amador, O.; Gaspariano, R.; Palma, R.; Munive, Z. Aliphatic, polycyclic aromatic hydrocarbons and nitrated polycyclic aromatic hydrocarbons in PM₁₀ in southwestern Mexico City. *Polycycl. Aromat. Compd.* **2008**, *28*, 578–597. [CrossRef]
- European Environment Agency. Persistent Organic Pollutant Emissions. Available online: <https://www.eea.europa.eu/data-and-maps/indicators/eea32-persistent-organic-pollutant-pop-emissions-1/assessment-10> (accessed on 25 May 2024).
- Famiyeh, L.; Chen, K.; Xu, J.; Sun, Y.; Guo, Q.; Wang, C.; Lv, J.; Tang, Y.T.; Yu, H.; Snape, C.; et al. A review on analysis methods, source identification, and cancer risk evaluation of atmospheric polycyclic aromatic hydrocarbons. *Sci. Total Environ.* **2021**, *789*, 147741. [CrossRef] [PubMed]
- Larsen, K.R.; Baker, J.E. Source Apportionment of Polycyclic Aromatic Hydrocarbons in the Urban Atmosphere: A Comparison of Three Methods. *Environ. Sci. Technol.* **2003**, *37*, 1873–1881. [CrossRef] [PubMed]
- Yang, B.; Zhou, L.; Xue, N.; Li, F.; Li, Y.; Vogt, R.D.; Cong, X.; Yan, Y.; Liu, B. Source apportionment of polycyclic aromatic hydrocarbons in soils of Huanghuai Plain, China: Comparison of three receptor models. *Sci. Total Environ.* **2013**, *443*, 31–39. [CrossRef] [PubMed]
- Lang, Y.H.; Li, G.L.; Wang, X.M.; Peng, P. Combination of Unmix and PMF receptor model to apportion the potential sources and contributions of PAHs in wetland soils from Jiaozhou Bay, China. *Mar. Pollut. Bull.* **2015**, *90*, 129–134. [CrossRef] [PubMed]
- Zhang, J.; Zhao, J.; Cai, J.; Gao, S.; Li, J.; Zeng, X.; Yu, Z. Spatial distribution and source apportionment of atmospheric polycyclic aromatic hydrocarbons in the Pearl River Delta. *China. Atmos. Pollut. Res.* **2018**, *9*, 887–893. [CrossRef]
- Wang, C.; Wu, S.; Zhou, S.; Wang, H.; Li, B.; Chen, H.; Yu, Y.; Shi, Y. Polycyclic aromatic hydrocarbons in soils from urban to rural areas in Nanjing: Concentration, source, spatial distribution, and potential human health risk. *Sci. Total Environ.* **2015**, *527–528*, 375–383. [CrossRef] [PubMed]
- Schifman, L.A.; Boving, T.B. Spatial and seasonal atmospheric PAH deposition patterns and sources in Rhode Island. *Atmos. Environ.* **2015**, *120*, 253–261. [CrossRef]
- Zhang, Y.; Lin, Y.; Cai, J.; Liu, Y.; Hong, L.; Qin, M.; Zhao, Y.; Ma, J.; Wang, X.; Zhu, T.; et al. Atmospheric PAHs in North China: Spatial distribution and sources. *Sci. Total Environ.* **2016**, *565*, 994–1000. [CrossRef]

14. Niu, S.; Liang, D.; Lifei, Z.; Chaofei, Z.; Reti, H.; Yeru, H. Temporal and spatial distribution, sources, and potential health risks of ambient polycyclic aromatic hydrocarbons in the Yangtze River Delta (YRD) of eastern China. *Chemosphere* **2017**, *172*, 72–79. [CrossRef]
15. Lim, S.S.; Vos, T.; Flaxman, A.D.; Danaei, G.; Shibuya, K.; Adair-Rohani, H.; AlMazroa, M.A.; Amann, M.; Anderson, H.R.; Andrews, K.G.; et al. A comparative risk assessment of burden of disease and injury attributable to 67 risk factors and risk factor clusters in 21 regions, 1990–2010: A systematic analysis for the Global Burden of Disease Study 2010. *Lancet* **2012**, *380*, 2224–2260. [CrossRef] [PubMed]
16. Hänninen, O.; Knol, A. *European Perspectives on Environmental Burden of Disease Estimates for Nine Stressors in Six European Countries*; National Institute for Health and Welfare (THL): Helsinki, Finland, 2011; ISBN 978-952-245-413-3.
17. Maertens, R.M.; Yang, X.; Zhu, J.; Gagne, R.W.; Douglas, G.R.; White, P.A. Mutagenic and carcinogenic hazards of settled house dust I: Polycyclic aromatic hydrocarbon content and excess lifetime cancer risk from preschool exposure. *Environ. Sci. Technol.* **2008**, *42*, 1747–1753. [CrossRef] [PubMed]
18. Collins, J.F.; Brown, J.P.; Alexeeff, G.V.; Salmon, A.G. Potency equivalency factors for some polycyclic aromatic hydrocarbons and polycyclic aromatic hydrocarbon derivatives. *Regul. Toxicol. Pharmacol.* **1998**, *28*, 45–54. [CrossRef] [PubMed]
19. Gao, P.; Guo, H.; Zhang, Z.; Ou, C.; Hang, J.; Fan, Q.; He, C.; Wu, B.; Feng, Y. Xing Bioaccessibility and exposure assessment of trace metals from urban airborne particulate matter (PM₁₀ and PM_{2.5}) in simulated digestive fluid. *Environ. Pollut.* **2018**, *242*, 1669–1677. [CrossRef] [PubMed]
20. Pachoulis, M.; Maggos, T.; Panagopoulos, P.; Dasopoulou, M.; Balla, D.; Stamatelopoulou, A.; Manousakas, M.I.; Eleftheriadis, K.; Saraga, D. Population Health Risks Assessment from Air Pollution Exposure in an Industrialized Residential Area in Greece. *Atmosphere* **2022**, *13*, 615. [CrossRef]
21. Vermillion Maier, M.L.; Siddens, L.K.; Pennington, J.M.; Uesugi, S.L.; Anderson, K.A.; Tidwell, L.G.; Tilton, S.C.; Ognibene, T.J.; Turteltaub, K.W.; Smith, J.N.; et al. Benzo[a]pyrene (BaP) metabolites predominant in human plasma following escalating oral micro-dosing with [¹⁴C]-BaP. *Environ. Int.* **2022**, *159*, 107045. [CrossRef] [PubMed]
22. Saraga, D.; Maggos, T.; Degrendele, C.; Klánová, J.; Horvat, M.; Kocman, D.; Kanduč, T.; Garcia Dos Santos, S.; Franco, R.; Gómez, P.M.; et al. Multi-city comparative PM_{2.5} source apportionment for fifteen sites in Europe: The ICARUS project. *Sci. Total Environ.* **2021**, *751*, 141855. [CrossRef] [PubMed]
23. Hopke, P.K.; Dai, Q.; Li, L.; Feng, Y. Global review of recent source apportionments for airborne particulate matter. *Sci. Total Environ.* **2020**, *740*, 140091. [CrossRef]
24. EN12341:2014; Ambient Air—Standard Gravimetric Measurement Method for the Determination of the PM₁₀ or PM_{2.5} Mass Concentration of Suspended Particulate Matter. European Committee for Standardization (CEN): Brussels, Belgium, 2014. Available online: <https://standards.iteh.ai/catalog/standards/cen/7ad508ad-33bd-4e41-942b-c52ddeb6d44d/en-12341-2014> (accessed on 26 May 2024).
25. Ravindra, K.; Sokhi, R.; Grieken, R.V. Atmospheric polycyclic aromatic hydrocarbons: Source attribution, emission factors and regulation. *Atmos. Environ.* **2008**, *42*, 2895–2921. [CrossRef]
26. Manoli, E.; Kouras, A.; Samara, C. Profile analysis of ambient and source emitted particle-bound polycyclic aromatic hydrocarbons from three sites in northern Greece. *Chemosphere* **2004**, *56*, 867–878. [CrossRef]
27. Mostert, M.M.R.; Ayoko, G.A.; Kokot, S. Application of chemometrics to analysis of soil pollutants. *TrAC Trends Anal. Chem.* **2010**, *29*, 430–445. [CrossRef]
28. Hwang, H.M.; Wade, T.L.; Sericano, J.L. Concentrations and source characterization of polycyclic aromatic hydrocarbons in pine needles from Korea, Mexico, and United States. *Atmos. Environ.* **2003**, *37*, 2259–2267. [CrossRef]
29. Tobiszewski, M.; Namieśnik, J. PAH diagnostic ratios for the identification of pollution emission sources. *Environ. Pollut.* **2012**, *162*, 110–119. [CrossRef]
30. Yunker, M.B.; Macdonald, R.W.; Vingarzan, R.; Mitchell, R.H.; Goyette, D.; Sylvestre, S. PAHs in the Fraser River basin: A critical appraisal of PAH ratios as indicators of PAH source and composition. *Org. Geochem.* **2002**, *33*, 489–515. [CrossRef]
31. Al-Nasir, F.; Hijazin, T.J.; Al-Alawi, M.M.; Jiries, A.; Al-Madanat, O.Y.; Mayyas, A.; Al-Dalain, S.A.; Al-Dmour, R.; Alahmad, A.; Batarseh, M.I. Accumulation, Source Identification, and Cancer Risk Assessment of Polycyclic Aromatic Hydrocarbons (PAHs) in Different Jordanian Vegetables. *Toxics* **2022**, *10*, 643. [CrossRef]
32. Duodu, G.O.; Ogogo, K.N.; Mummullage, S.; Harden, F.; Goonetilleke, A.; Ayoko, G.A. Source apportionment and risk assessment of PAHs in Brisbane River sediment, Australia. *Ecol. Indic.* **2017**, *73*, 784–799. [CrossRef]
33. Inam, E.; Offiong, N.A.; Essien, J.; Kang, S.; Kang, S.Y.; Antia, B. Polycyclic aromatic hydrocarbons loads and potential risks in freshwater ecosystem of the Ikpa River Basin, Niger Delta—Nigeria. *Environ. Monit. Assess.* **2016**, *188*, 49. [CrossRef]
34. Capozzi, F.; Adamo, P.; Spagnuolo, V.; Giordano, S. Field comparison between moss and lichen PAHs uptake abilities based on deposition fluxes and diagnostic ratios. *Ecol. Indic.* **2021**, *120*, 106954. [CrossRef]
35. Bootdee, S.; Chantara, S.; Prapamontol, T. Determination of PM_{2.5} and polycyclic aromatic hydrocarbons from incense burning mission at shrine for health risk assessment. *Atmos. Pollut. Res.* **2016**, *7*, 680–689. [CrossRef]
36. Paatero, P.; Tappert, U. Positive matrix factorization: A non-negative factor model with optimal utilization of error estimates odd data values. *Environmetrics* **1994**, *5*, 111–126. [CrossRef]

37. Degrendele, C.; Fiedler, H.; Kočan, A.; Kukučka, P.; Přibylková, P.; Prokeš, R.; Klánová, J.; Lammel, G. Multiyear levels of PCDD/Fs, dl-PCBs and PAHs in background air in central Europe and implications for deposition. *Chemosphere* **2020**, *240*, 124852. [[CrossRef](#)] [[PubMed](#)]
38. Polissar, A.V.; Hopke, P.K.; Poirot, R.L. Atmospheric aerosol over Vermont: Chemical composition and sources. *Environ. Sci. Technol.* **2001**, *35*, 4604–4621. [[CrossRef](#)] [[PubMed](#)]
39. Mircea, M.; Calori, G.; Pirovano, G.; Belis, C. *European Guide on Air Pollution Source Apportionment for Particulate Matter with Source Oriented Models and Their Combined Use with Receptor Models*, EUR 30082 EN; Publications Office of the European Union: Luxembourg, 2020; Volume 2020, ISBN 978-92-76-10698-2. [[CrossRef](#)]
40. Norris, G.A.; Paatero, P.; Eberly, S.; Brown, S.G. Methods for estimating uncertainty in factor analytic solutions. *Atmos. Meas.* **2014**, *7*, 781–797. [[CrossRef](#)]
41. Jackson, M.M. Roadside concentration of gaseous and particulate matter pollutants and risk assessment in dar-Es-Salaam, Tanzania. *Environ. Monit. Assess.* **2005**, *104*, 385–407. [[CrossRef](#)] [[PubMed](#)]
42. Farris, F.F.; Ray, S.D. Cancer Potency Factor. *Encycl. Toxicol. Third Ed.* **2014**, *1*, 642–644. [[CrossRef](#)]
43. International Commission on Radiological Protection (ICRP). *Basic Anatomical and Physiological Data for Use in Radiological Protection: Reference Values*; Valentin, J., Ed.; International Commission on Radiological Protection: Stockholm, Sweden, 2002; Volume 32, ISBN 008 0442668. Available online: <http://www.icrp.org/publication.asp?id=icrp%20publication%2089> (accessed on 26 May 2024).
44. Office of Environmental Health Hazard Assessment (OEHHA). Air Toxics Hot Spots Program. In *Guidance Manual for Preparation of Health Risk Assessment*; California Environmental Protection Agency U.S.: Sacramento, CA, USA, 2015; p. 231. Available online: http://oehha.ca.gov/air/hot_spots/2015/2015GuidanceManual.pdf (accessed on 26 May 2024).
45. U.S. Environmental Protection Agency. *Exposure Factors Handbook*; National Center for Environmental Assessment: Washington, DC, USA, 2011.
46. U.S. EPA. Regional Screening Level (RSL) Summary Table. 2019. Available online: <https://www.epa.gov/risk/regionalscreening-levels-rsls-generic-tables> (accessed on 26 May 2024).
47. Nisbet, I.C.T.; Lagoy, P.K. Toxic Equivalency Factors (TEFs) for Polycyclic Aromatic Hydrocarbons (PAHs). *Regul. Toxicol. Pharmacol.* **1992**, *16*, 290–300. [[CrossRef](#)] [[PubMed](#)]
48. OEHHA. *Air Toxics Hot Spots Program Risk Assessment Guidelines*; California Environmental Protection Agency, Office of Environmental Health Hazard Assessment, Air Toxicology and Epidemiology Section: Oakland, CA, USA, 2005.
49. World Health Organization. *WHO Guidelines for Indoor Air Quality: Selected Pollutants*; Regional Office for Europe: København, Denmark, 2010; Available online: <https://apps.who.int/iris/handle/10665/260127> (accessed on 26 May 2024).
50. Halek, F.; Nabi, G.; Kavousi, A. Polycyclic aromatic hydrocarbons study and toxic equivalency factor (TEFs) in Tehran, Iran. *Environ. Monit. Assess.* **2008**, *143*, 303–311. [[CrossRef](#)] [[PubMed](#)]
51. Hong, H.S.; Yin, H.L.; Wang, X.H.; Ye, C.X. Seasonal variation of PM10-bound PAHs in the atmosphere of Xiamen, China. *Atmos. Res.* **2007**, *85*, 429–441. [[CrossRef](#)]
52. León-Camacho, M.; Viera-Alcaide, I.; Ruiz-Méndez, M.V. Elimination of polycyclic aromatic hydrocarbons by bleaching of olive pomace oil. *Eur. J. Lipid Sci. Technol.* **2003**, *105*, 9–16. [[CrossRef](#)]
53. Guillén, M.D.; Sopelana, P.; Palencia, G. Polycyclic Aromatic Hydrocarbons and Olive Pomace Oil. *J. Agric. Food Chem.* **2004**, *52*, 2123–2132. [[CrossRef](#)]
54. Mantis, J.; Chaloulakou, A.; Samara, C. PM₁₀-bound polycyclic aromatic hydrocarbons (PAHs) in the Greater Area of Athens, Greece. *Chemosphere* **2005**, *59*, 593–604. [[CrossRef](#)]
55. Fang, G.C.; Wu, Y.S.; Chen, J.C.; Cheng Fu, P.P.; Chang, C.N.; Ho, T.T.; Chen, M.H. Characteristic study of polycyclic aromatic hydrocarbons for fine and coarse particulates at Pastureland near Industrial Park sampling site of central Taiwan. *Chemosphere* **2005**, *60*, 427–433. [[CrossRef](#)] [[PubMed](#)]
56. Pateraki, S.; Fameli, K.-M.; Assimakopoulos, V.; Bairachtari, K.; Zagkos, A.; Stavrika, T.; Bougiatioti, A.; Maggos, T.; Mihalopoulos, N. Differentiation of the Athens Fine PM Profile during Economic Recession (March of 2008 Versus March of 2013): Impact of Changes in Anthropogenic Emissions and the Associated Health Effect. *Atmosphere* **2020**, *11*, 1121. [[CrossRef](#)]
57. Valerio, F.; Pala, M.; Lazzarotto, A.; Stella, A.; Ciccarelli, F.; Balducci, D.; Brescianini, C. Air Quality Standard for Benzo(a)pyrene (BaP) in Genoa (1994–1995). *Polycycl. Aromat. Compd.* **1996**, *9*, 61–66. [[CrossRef](#)]
58. Brown, J.R.; Field, R.A.; Goldstone, M.E.; Lester, J.N.; Perry, R. Polycyclic aromatic hydrocarbons in central London air during 1991 and 1992. *Sci. Total Environ.* **1996**, *177*, 73–84. [[CrossRef](#)] [[PubMed](#)]
59. Andreassen, Å.; Kure, E.H.; Nielsen, P.S.; Autrup, H.; Haugen, A. Comparative synchronous fluorescence spectrophotometry and 32P-postlabelling analysis of PAH-DNA adducts in human lung and the relationship to TP53 mutations. *Mutat. Res./Genet. Toxicol.* **1996**, *368*, 275–282. [[CrossRef](#)]
60. Theodosi, C.; Grivas, G.; Zarnmpas, P.; Chaloulakou, A.; Mihalopoulos, N. Mass and chemical composition of size-segregated aerosols (PM₁, PM_{2.5}, PM₁₀) over Athens, Greece: Local versus regional sources. *Atmos. Chem. Phys.* **2011**, *11*, 11895–11911. [[CrossRef](#)]
61. Masiol, M.; Hofer, A.; Squizzato, S.; Piazza, R.; Rampazzo, G.; Pavoni, B. Source apportionment of PM_{2.5} at multiple sites in Venice (Italy): Spatial variability and the role of weather. *Atmos. Environ.* **2014**, *98*, 78–88. [[CrossRef](#)]

62. Hanedar, A.; Alp, K.; Kaynak, B.; Baek, J.; Avsar, E.; Odman, M.T. Concentrations and sources of PAHs at three stations in Istanbul, Turkey. *Atmos. Res.* **2011**, *99*, 391–399. [[CrossRef](#)]
63. El Haddad, I.; Marchand, N.; Wortham, H.; Piot, C.; Besombes, J.L.; Cozic, J.; Chauvel, C.; Armengaud, A.; Robin, D.; Jaffrezo, J.L. Primary sources of PM_{2.5} organic aerosol in an industrial Mediterranean city, Marseille. *Atmos. Chem. Phys.* **2011**, *11*, 2039–2058. [[CrossRef](#)]
64. Amato, F.; Pandolfi, M.; Moreno, T.; Furger, M.; Pey, J.; Alastuey, A.; Bukowiecki, N.; Prevot, A.S.H.; Baltensperger, U.; Querol, X.; et al. Sources and variability of inhalable road dust particles in three European cities. *Atmos. Environ.* **2011**, *45*, 6777–6787. [[CrossRef](#)]
65. Waked, A.; Favez, O.; Alleman, L.Y.; Piot, C.; Petit, J.-E.; Delaunay, T.; Verlinden, E.; Golly, B.; Jaffrezo, J.-L.; Leoz-Garziandia, E.; et al. Source apportionment of PM₁₀ in a north-western Europe regional urban background site (Lens, France) using positive matrix factorization and including primary biogenic emissions. *Atmos. Chem. Phys.* **2014**, *14*, 3325–3346. [[CrossRef](#)]
66. Salameh, D.; Detournay, A.; Pey, J.; Pérez, N.; Liguori, F.; Saraga, D.; Bove, M.C.; Brotto, P.; Cassola, F.; Massabò, D.; et al. PM_{2.5} chemical composition in five European Mediterranean cities: A 1-year study. *Atmos. Res.* **2015**, *155*, 102–117. [[CrossRef](#)]
67. Argyropoulos, G.; Samara, C.; Diapouli, E.; Eleftheriadis, K.; Papaioikonomou, K.; Kungolos, A. Source apportionment of PM₁₀ and PM_{2.5} in major urban Greek agglomerations using a hybrid source-receptor modeling process. *Sci. Total Environ.* **2017**, *601–602*, 906–917. [[CrossRef](#)] [[PubMed](#)]
68. Saraga, D.E.; Makrogkika, A.; Karavoltzos, S.; Sakellari, A.; Diapouli, E.; Eleftheriadis, K.; Vasilakos, C.; Helmis, C.; Maggos, T. A Pilot Investigation of PM Indoor/Outdoor Mass Concentration and Chemical Analysis during a Period of Extensive Fireplace Use in Athens. *Aerosol Air Qual. Res.* **2015**, *15*, 2485–2495. [[CrossRef](#)]
69. Hassan, H.; Saraga, D.; Kumar, P.; Kakosimos, K.E. Vehicle-induced fugitive particulate matter emissions in a city of arid desert climate. *Atmos. Environ.* **2020**, *229*, 117450. [[CrossRef](#)]
70. Lucarelli, F.; Mandò, P.A.; Nava, S.; Prati, P.; Zucchiatti, A. One-Year Study of the Elemental Composition and Source Apportionment of PM₁₀ Aerosols in Florence, Italy. *J. Air Waste Manag. Assoc.* **2004**, *54*, 1372–1382. [[CrossRef](#)]

Disclaimer/Publisher’s Note: The statements, opinions and data contained in all publications are solely those of the individual author(s) and contributor(s) and not of MDPI and/or the editor(s). MDPI and/or the editor(s) disclaim responsibility for any injury to people or property resulting from any ideas, methods, instructions or products referred to in the content.